Larger amounts of precipitate were obtained from Test #1, which allowed for more analyses. X-ray fluorescence (XRF) was another procedure used to determine the elemental composition of the precipitates from Test #1, and the results are available in the Test #1 data report (Ref. 2). The results indicated that the Test #1 precipitates were mainly composed of Na, Al, Ca, and Si. The accuracy of the results depends on how closely the comparative standards resemble the sample. Also, the sensitivity of XRF decreases with decreasing atomic weight, so it is normally difficult to identify an element with an atomic number that is less than that of carbon. Since boron cannot be detected by XRF, the elemental composition obtained from this procedure was in agreement with that obtained from the ICP-AES analysis.

ICP-AES and XRF analyses provided an elemental composition of the Test #1 precipitate, but did not offer any information about the structure. Analytical procedures, which include TEM and x-ray diffraction (XRD) analyses, were used to aid with further characterization of the precipitate obtained from Test #1 (Ref. 2). These procedures were mainly used to determine whether the solids physical structure was more consistent with microcrystalline flocculent or with amorphous hydrated gels. Upon examination of the results, it is likely that the precipitate was amorphous in nature.

4.2. Insulation

In this section, post-test examinations of fiberglass (Section 4.2.1) and cal-sil (Section 4.2.2) are presented.

4.2.1. Fiberglass

Fiberglass insulation was present in the tank in each test. In the fiberglass-only tests (Tests #1, #2, and #5) there was 4.58 ft^3 of shredded fiberglass in the tank. In Tests #3 and #4, there was 80% of that amount in the tank. In all of the tests, 75% of the fiberglass was submerged. Most of the submerged fiberglass was bundled in 3-in.-thick bags (or blankets) of fiberglass confined in SS mesh to prevent ingestion through the pump and to better control the placement of fiberglass in various flow regimes. Those blankets rested on the tank bottom, away from the tank drain. Other fiberglass samples were designated by their placement in high-flow and low-flow regions of the tank. In high-flow regions, the smaller blankets were attached to the submerged coupon rack (Figure 2-4), and they were exposed to direct flow from the recirculation flow headers. Blankets in low-flow regions did not experience direct water flow. Additional 4-in.-square envelopes of fiberglass (Figure 2-4) were also prepared for extraction during the course of the test. These samples were referred to as “sacrificial” samples. One sample, called the “birdcage,” was constructed so that the fiberglass within it was loose and not compacted. The birdcage fiberglass sat on the tank bottom and was removed on Day 30. Also, a cylindrical blanket of fiberglass was placed around the tank drain screen. The unsubmerged fiberglass was placed in blankets and attached to the ends of suspended coupon racks. Some amount of fiber, especially short-fiber fragments, escaped the mesh bags and was deposited in other locations within the tank. This material was referred to as “fugitive” fiberglass.

An SEM image of clean fiberglass, before exposure to the test solution, is shown in Figure 4-17. This SEM image provides a visual baseline as a comparison for images from samples taken after the tests began. As can be seen, there are no deposits on the clean fiberglass. Over the course of each test, deposits were observed throughout the fiberglass samples. These deposits could be of chemical origin (i.e., solids that formed at the surface of the fiberglass because of chemical reactions between soluble chemical species and the fiberglass or because of precipitation of soluble species at that location) or physically retained or attached (i.e., deposits that existed as solid particles in the test solution and were captured by the fiberglass). Because there was not significant water flow through the fiber, particle migration into the fiberglass interior was not likely; however, physical retention and attachment of particles at the exterior of fiberglass were possible. Therefore, deposits found in the interior of the fiberglass samples were likely of chemical origin, whereas the deposits on the exterior could have been of either origin.

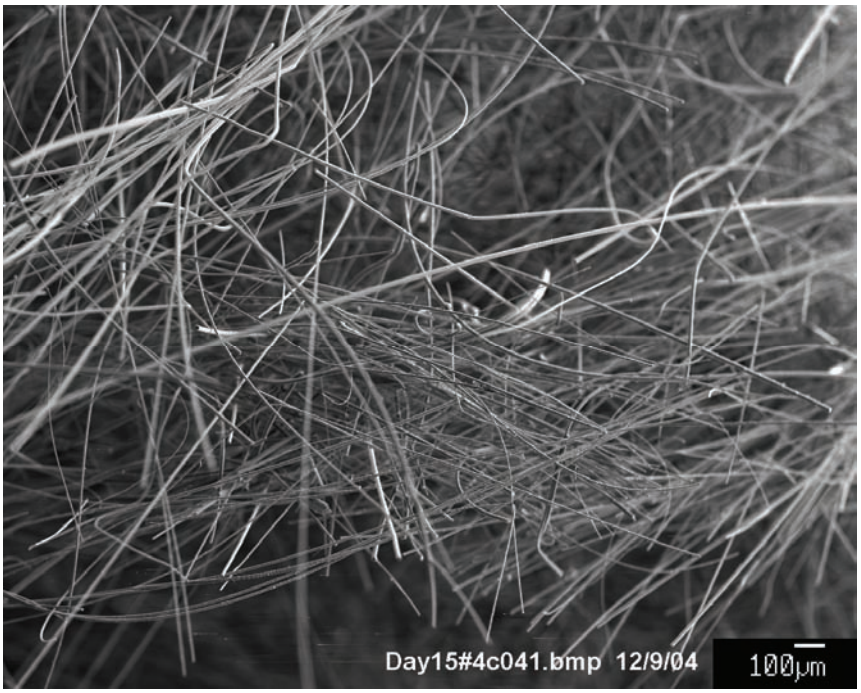

Figure 4-17. Clean fiberglass before exposure to test chemicals.

The amount of deposits varied between tests because of the differences in the chemical conditions. In some tests (Tests #1, #2, and #5), fiberglass was the only insulation material present, whereas in the other tests (Tests #3 and #4), the insulation present was a mixture of 20% fiberglass and 80% cal-sil (by volume). In addition, the chemicals used and the test pH varied between tests. The pertinent test conditions, insulation type, relative amounts of deposits in each test, and likely sources of deposits are summarized in Table 4-5. In addition to differences between tests, a time dependence of the deposits was observed, with the amount of deposits increasing as each test proceeded. Test #5 was an exception, where time dependence of the deposits was insignificant. Furthermore, differences between fiberglass sample locations within the tank were observed; the general trend was that the amount of deposits was greatest on the drain collar's outside exterior (farthest from the drain screen), followed by the drain collar's inside exterior (next to the drain screen), followed by the birdcage exterior, and then followed by

the high-flow fiberglass exterior. Descriptions of the deposits observed in each test are detailed in the following sections.

Table 4-5. Relative Amounts of Particle Deposits in Fiberglass

Test	pH and Chemicals[a]	Insulation	Likely Sources
1	pH = 9.3 to 9.5 H_3BO_3 = 2,800 mg/L NaOH = 8,021 mg/L	100% fiberglass	High pH caused severe corrosion on aluminum. Corrosion products then precipitated on the fiberglass.
2	pH = 7.1 to 7.4 H_3BO_3 = 2,800 mg/L TSP = 4,000 mg/L	100% fiberglass	Low pH caused less corrosion; however, TSP may have formed precipitates.
3	pH = 7.3 to 8.1 H_3BO_3 = 2,800 mg/L TSP = 4,000 mg/L	20% fiberglass 80% cal-sil	TSP reacted with calcium from the cal-sil and formed calcium phosphate precipitates. In addition, flowing water suspended some of the cal-sil debris, which then deposited on the fiberglass. Cal-sil deposits were observed on the exterior surface and the amount of deposits was more than in Tests #1 and #2.
4	pH = 9.5 to 9.9 H_3BO_3 = 2,800 mg/L NaOH = 8,951 mg/L	20% fiberglass 80% cal-sil	Cal-sil debris was suspended by the flowing water and deposited on the fiberglass. Corrosion was lower, possibly because of passivation of the metal coupon surfaces by silicate that originated from the cal-sil. Cal-sil deposits were observed on the exterior surface, and the amount of deposits was more than in Tests #1 and #2.
5	pH = 8.2 to 8.5 H_3BO_3 = 6,848 mg/L Borax = 10,568 mg/L	100% fiberglass	Low corrosion and insignificant chemical precipitation. The amount of deposits was less than in Tests #1 and #2.

[a] H_3BO_3 is reported in milligrams per liter as boron, TSP is reported in milligrams per liter as $Na_3PO_4 \cdot 12H_2O$, borax is reported in milligrams per liter as $Na_2B_4O_7 \cdot 10H_2O$. Additional chemicals were present in the test solution (see Table A-4).

Test #1

In Test #1, the most significant deposits observed on the fiberglass were thin crusts, as shown in Figure 4-18, and sheets of film (i.e., webbing) that stretched between multiple fibers, as shown in Figures 4-19 and 4-20. In these SEM images, it is important to note that all samples were partially or thoroughly desiccated before examination, which may have contributed to the cracking of the webbing shown in Figure 4-19. The EDS analysis shown in Figure 4-21 indicates that the thin crusts were composed primarily of sodium, aluminum, silicon, and oxygen, whereas the webbing was primarily composed of sodium, boron, and oxygen, as shown in Figure 4-22.

Lab diagnostic tests revealed that the webbing material was likely an artifact of the sampling and analysis procedure and may not have existed when the fiberglass was submerged in the tank. On removal from the tank, the fiberglass was wet with the tank solution, and it appears that the webbing formed as the tank solution evaporated. A sample of clean fiberglass dipped momentarily in the ICET Test #1 solution and allowed to dry exhibited similar webbing, as shown in Figure 4-23. Moreover, the EDS analysis of this webbing (shown in Figure 4-24) indicated that the webbing produced in bench-top experiments exhibited elemental composition similar to the webbing observed in the Test #1 fiberglass (the silicon peak is likely from the fiberglass in the background of the webbing). This webbing was not observed when a sample of clean fiberglass was dipped momentarily in the ICET Test #1 solution, rinsed gently with RO water, and allowed to dry, as shown in Figure 4-25, thus demonstrating that the residual liquid on the surface of the fiberglass was responsible for film formation and that the webbing was actually soluble. Additional diagnostic tests indicated that sodium hydroxide did not contribute to the formation of webbing material (see Figure 4-26). However, a sodium borate solution at pH 9.5 did result in webbing on the fiberglass (see Figures 4-27 and 4-28). The elemental composition of the webbing after it was dipped in sodium borate, as shown in Figure 4-29 was consistent with the elemental composition after it was dipped in the ICET Test #1 solution (see Figure 4-24).

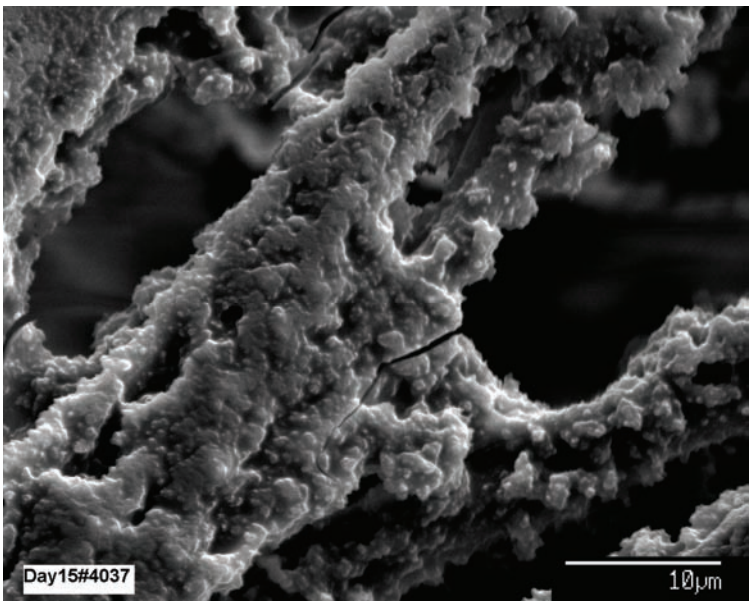

Figure 4-18. Day 15, sample #4 SEM image (#4037), magnified 2500 times; BSE close-up.

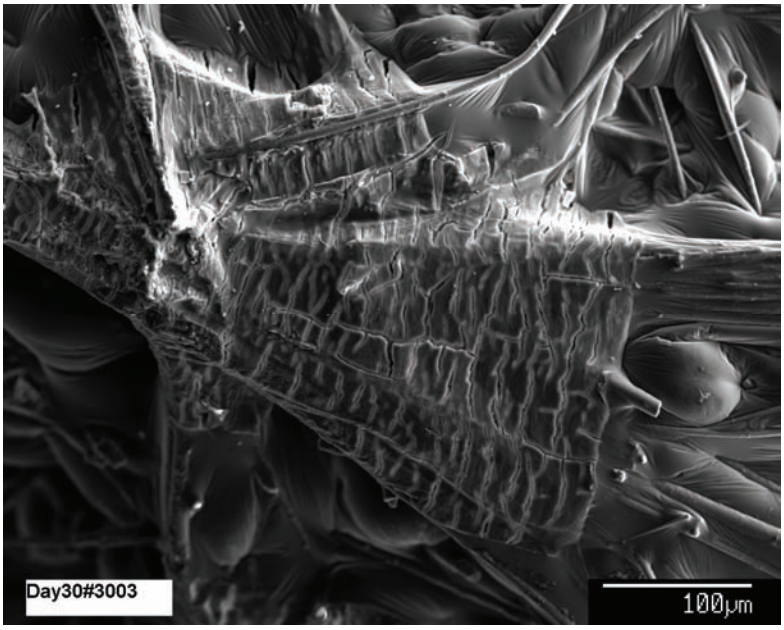

Figure 4-19. Day 30, sample #3 SEM image (#3003), magnified 250 times, of the fiberglass with surface coating.

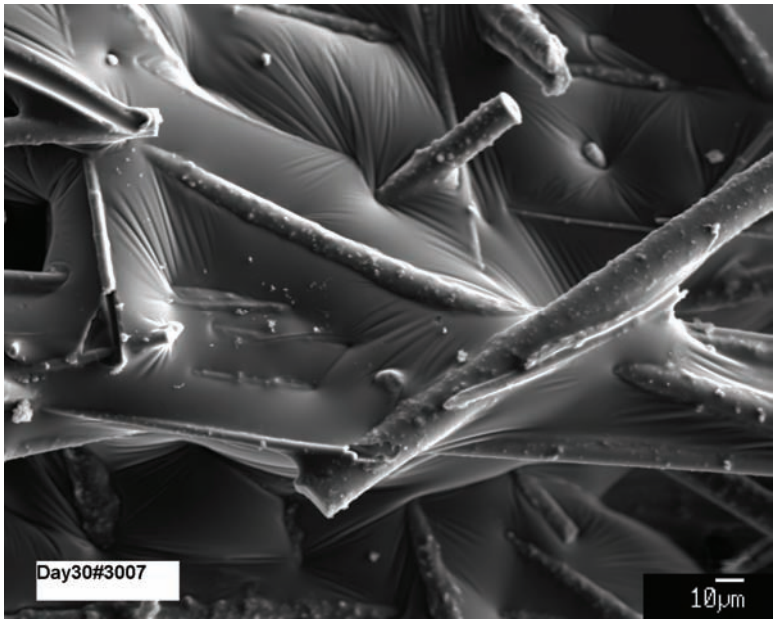

Figure 4-20. Day 30, sample #3 SEM image (#3007), magnified 500 times, of the film across the fibers.

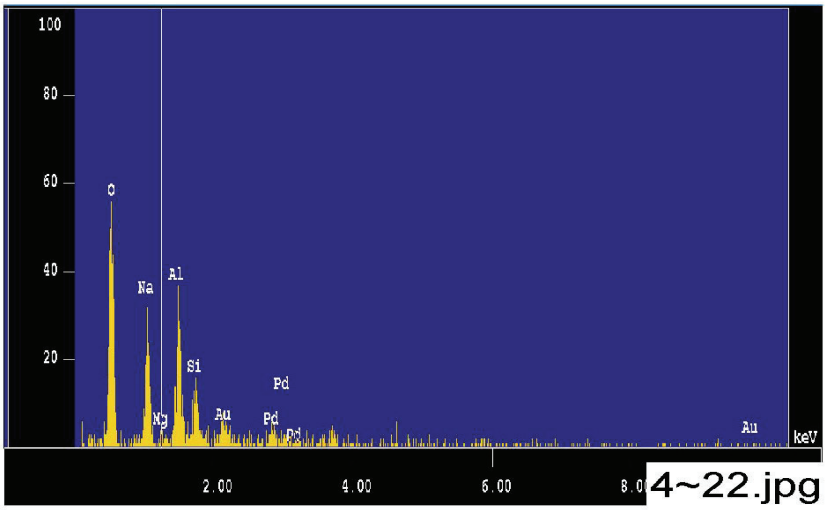

Figure 4-21. Day 15, sample #4 counting spectrum (EDS 4-22) for the crust on the fiberglass, as shown in Figure 4-18.

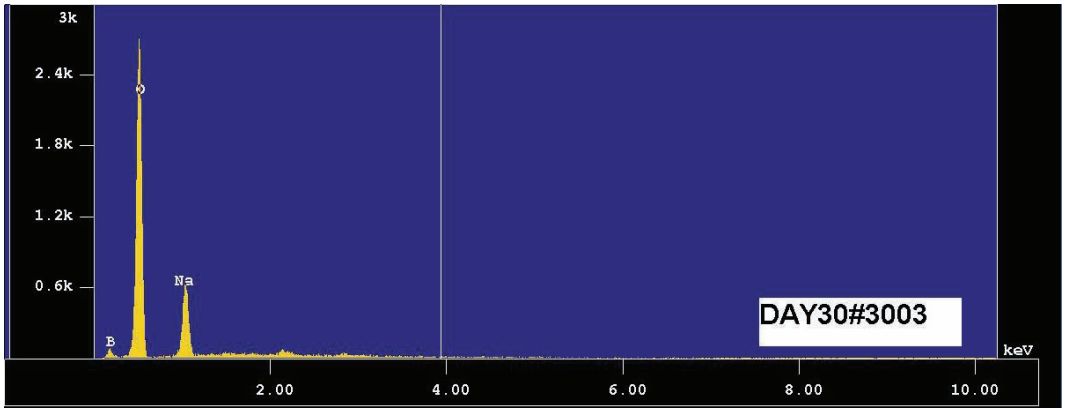

Figure 4-22. Day 30, sample #3 counting spectrum (EDS #3003) of the fractured coating, as shown in Figure 4-19.

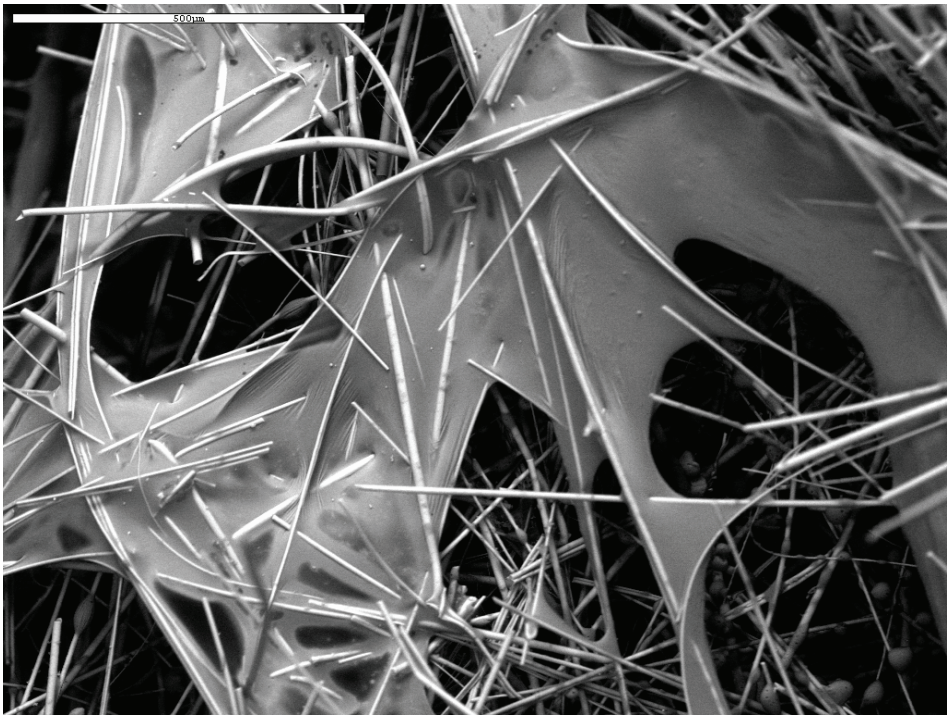

Figure 4-23. ESEM image, magnified 100 times, of raw fiberglass dipped in ICET Test #1 solution. (rfbt105.tif, 7/28/05)

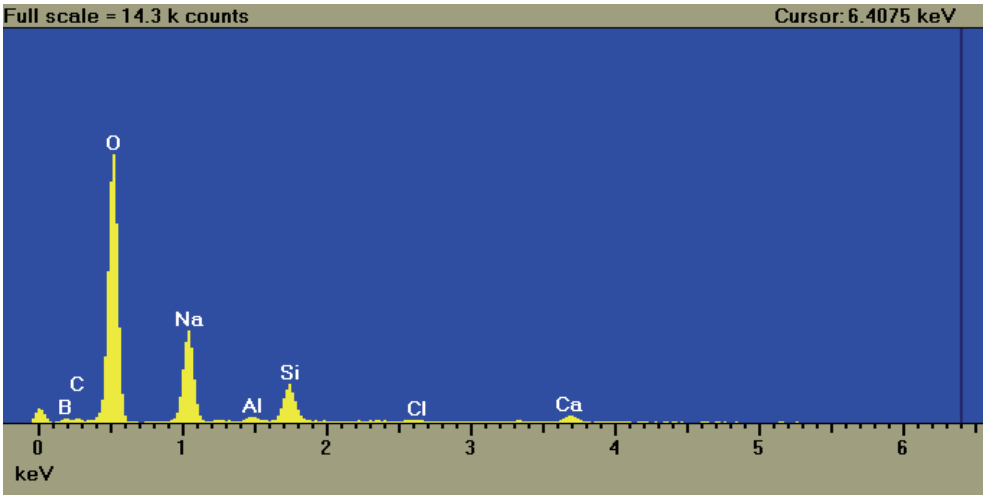

Figure 4-24. EDS counting spectrum for the film on fiberglass, as shown in Figure 4-23. (rfbt106.tif, 7/28/05)

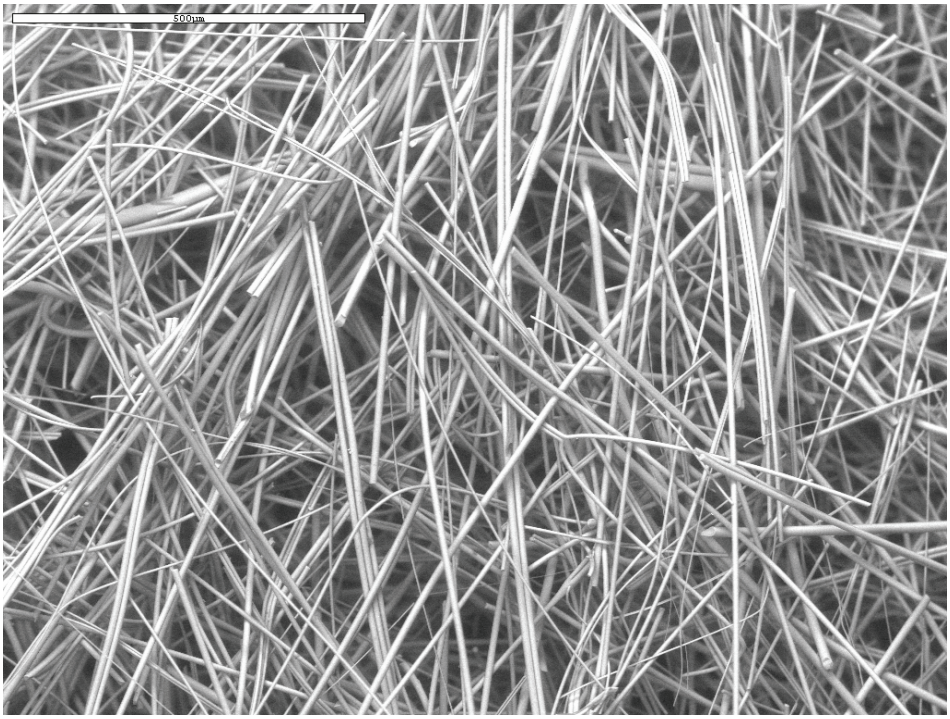

Figure 4-25. ESEM image, magnified 100 times, of raw fiberglass dipped in ICET Test #1 solution and then washed with RO water. (DIfbrg15.tif, 8/3/05)

Figure 4-26. ESEM image, magnified 100 times, of raw fiberglass dipped in NaOH solution at pH 9.5. (OHFbrg07.tif, 8/3/05)

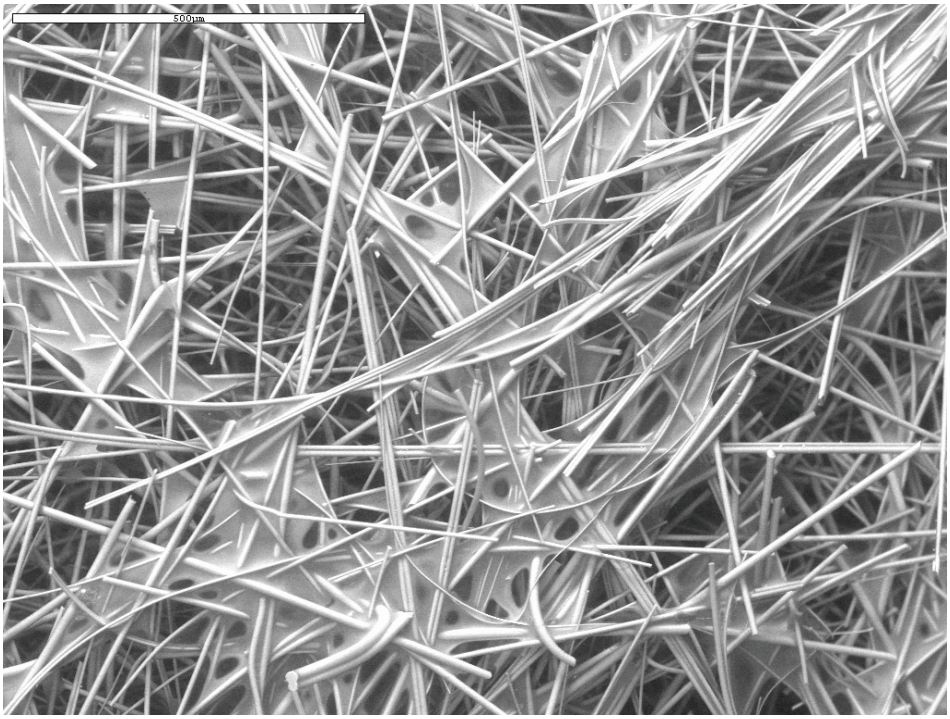

Figure 4-27. ESEM image, magnified 100 times, of raw fiberglass dipped in the solution containing 2800 mg/L boron and NaOH at pH 9.5. (Bofbrg09.tif, 8/3/05)

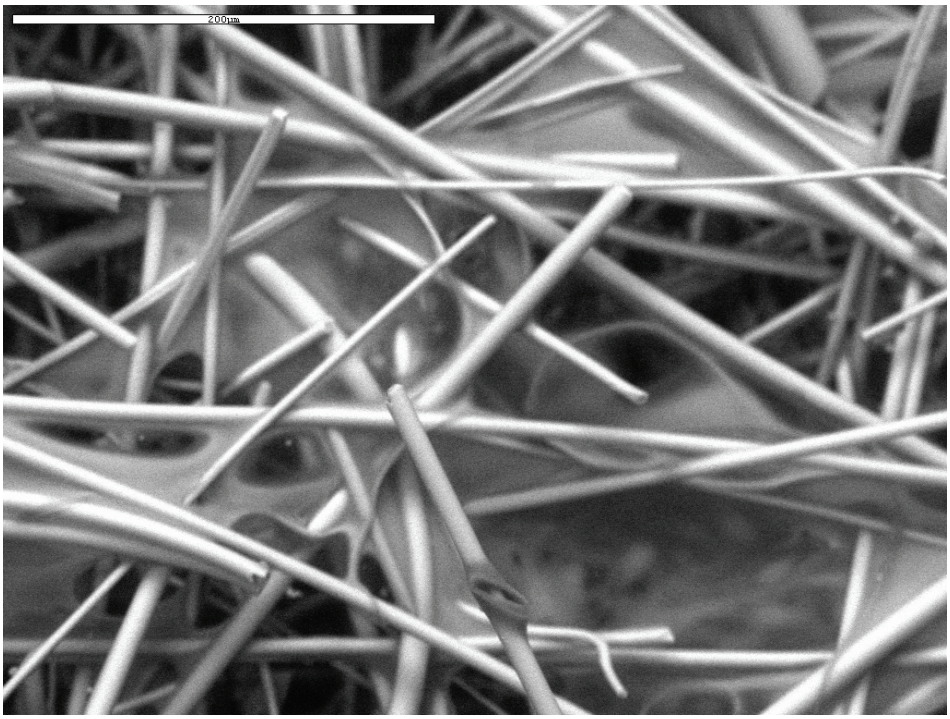

Figure 4-28. ESEM image, magnified 300 times, of raw fiberglass dipped in the solution containing 2800 mg/L boron and NaOH at pH 9.5. (rfbgbn03.tif, 8/5/05)

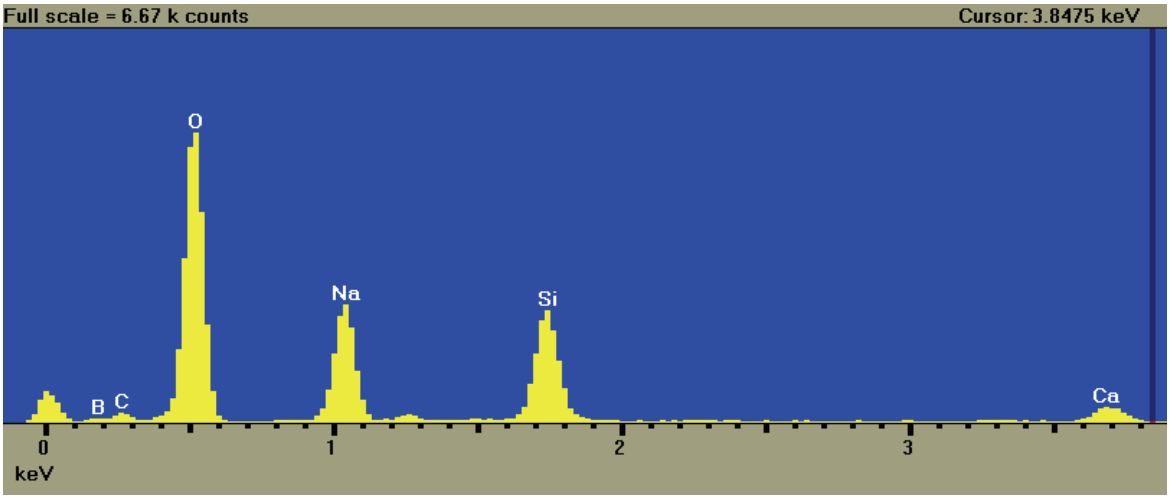

Figure 4-29. EDS counting spectrum for the film on fiberglass, as shown in Figure 4-28. (rfbgbn05.tif, 8/5/05)

Test #2

Fiberglass samples from four locations in the tank were examined in Test #2, including the low-flow area, high-flow area, birdcage, and drain collar. Both the interior and exterior regions of the fiberglass samples were examined in each location. In general, the amount of deposits increased as the test proceeded. Figures 4-30 through 4-33 show deposits in the interior and exterior regions of the high-flow, Day-30 fiberglass samples. The figures show that the deposits were pervasive throughout the fiberglass. However, the particulate deposits were more significant in the exterior fiberglass samples, whereas flocculent deposits were more prevalent in the interior fiberglass samples. When the probe SEM results were compared with the ESEM results, more significant flocculent deposits were found with probe SEM analysis (compare Figures 4-33 and 4-34, which are at approximately the same magnification), especially for the interior fiberglass samples. The possible reason is that ESEM samples were moist compared with the dry-probe SEM samples during the examination process, and the drying process may have caused the formation of the flocculent deposits, i.e., chemical precipitation. However, it is also possible that the flocculent deposits are chemical byproducts formed during the test. In addition, the EDS results from Figure 4-35 indicate numerous elemental constituents in these deposits, including oxygen, sodium, aluminum, phosphorus, calcium, and possibly silicon. These elements likely originated from the metal and concrete coupons, fiberglass, and testing solution.

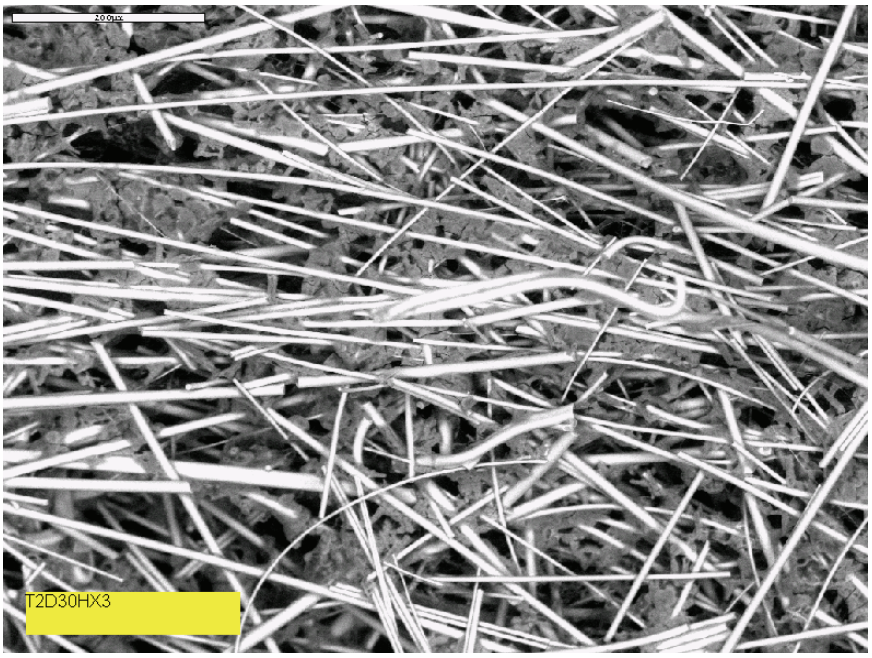

Figure 4-30. ESEM image for a Test #2, Day 30, high-flow exterior fiberglass sample.

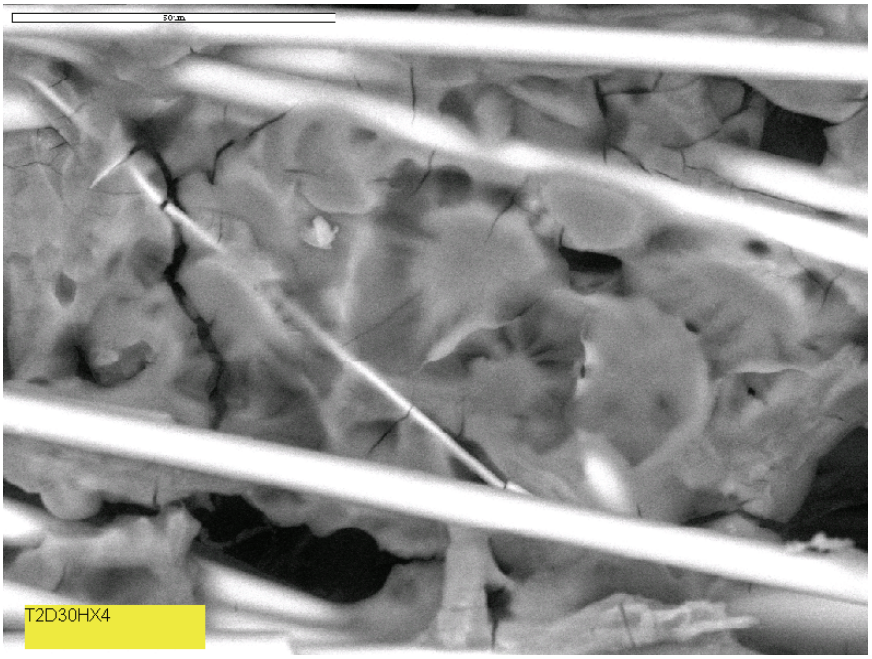

Figure 4-31. Higher-magnification ESEM image of a Test #2, Day 30, high-flow exterior fiberglass sample.

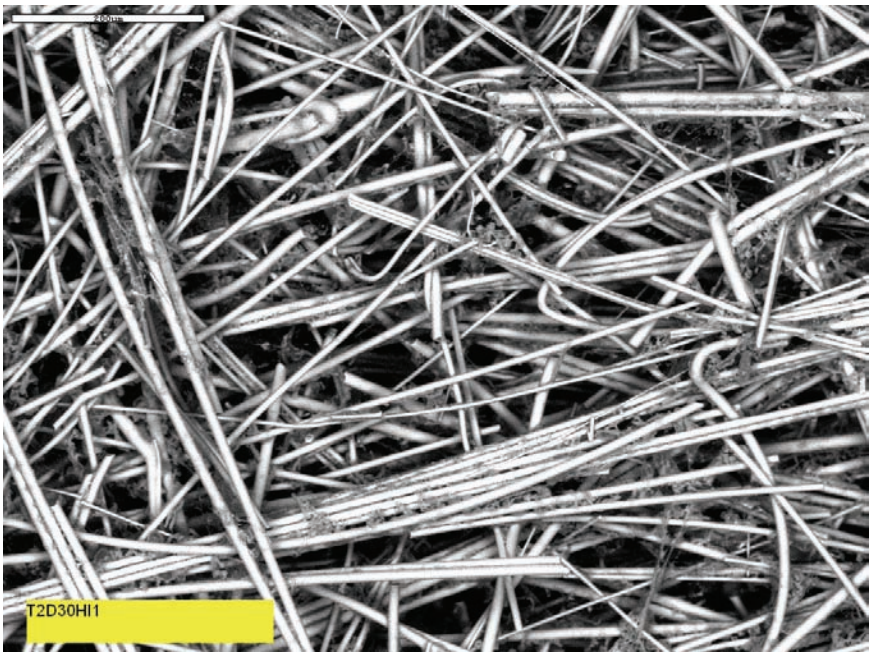

Figure 4-32. ESEM image for a Test #2, Day 30, high-flow interior fiberglass sample.

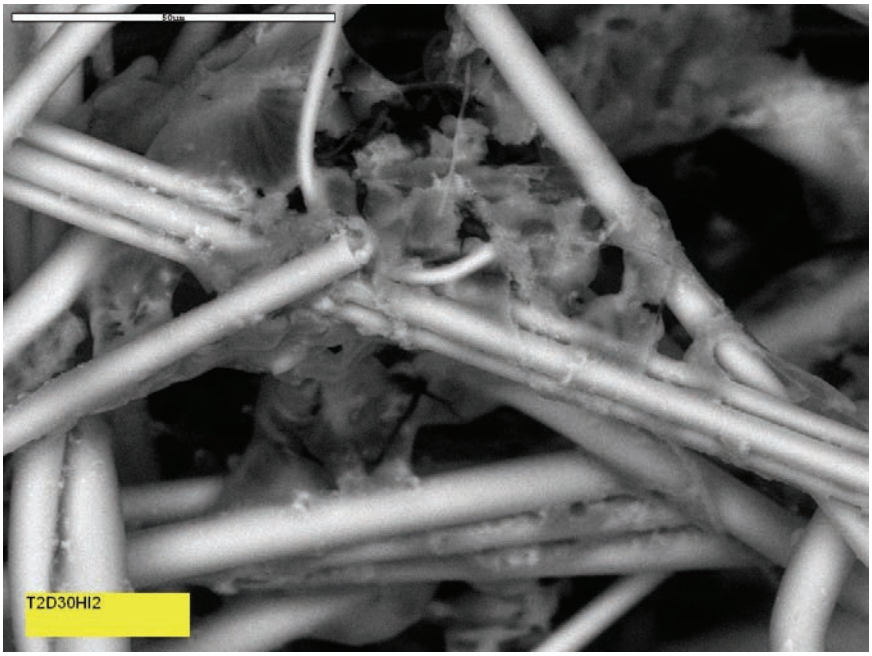

Figure 4-33. Higher-magnification ESEM image of a Test #2, Day 30, high-flow interior fiberglass sample.

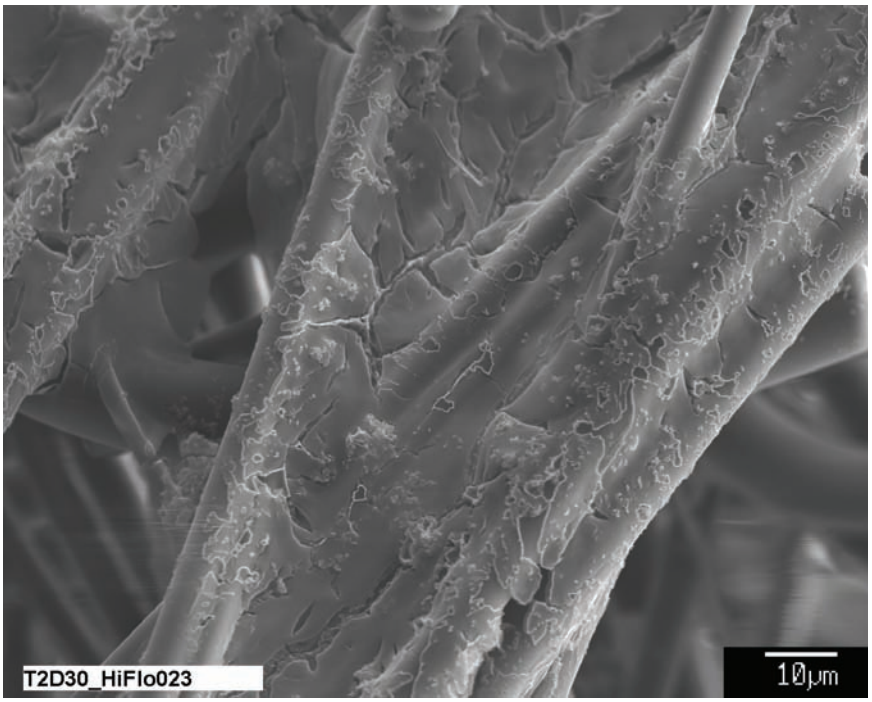

Figure 4-34. Probe SEM image at 1000× magnification for a Test #2, Day 30, high-flow interior fiberglass sample. (T2D30_HiFlo023)

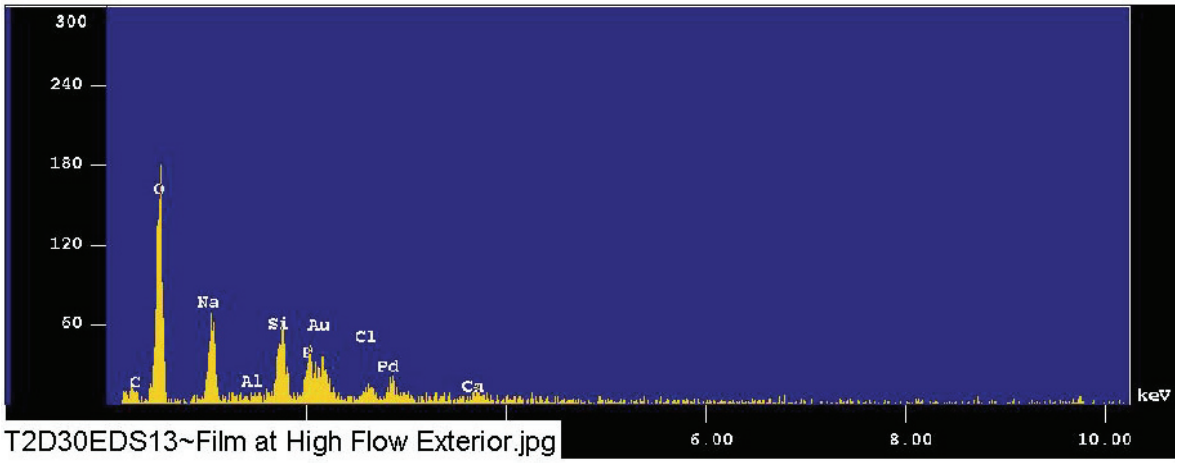

Figure 4-35. EDS counting spectrum for the deposits on a high-flow exterior fiberglass sample.

Test #3

Tests #3 and Test #4 each had much greater amounts of deposits than Tests #1, #2, and #5. In addition, the amount of deposits increased as the test proceeded. The greatest amount of deposits was found on the exteriors of the Day-30 samples, as shown in Figure 4-36. The corresponding EDS is shown in Figure 4-37. Based on EDS analysis, the particulate deposits on the fiberglass exterior may be divided into two categories according to phosphorus and silicon content, as shown in Figures 4-38 and 4-39. Particulate deposits of lower phosphorus and higher silicon content were likely cal-sil particles. The particulate deposits with lower silicon and high phosphorus, calcium, and oxygen content were likely composed of calcium phosphate precipitates, and it is compositionally similar to the white gel found on the tank bottom at the end of the test. It is likely that calcium and phosphate precipitated when dissolved calcium from the cal-sil reacted with phosphate from the TSP. After precipitation, the calcium phosphate precipitates were transported to the fiberglass exterior by sedimentation and/or water flow depending on the location of the fiberglass sample within the tank. Both kinds of deposits (cal-sil and calcium phosphate precipitates) may be physically transported and/or deposited onto the fiberglass sample exterior in this manner.

In contrast to the exterior regions of the fiberglass, the interior fiberglass samples were relatively pristine, as shown in Figures 4-40 and 4-41. These results suggest that almost all of the particulate deposits were physically retained at the fiberglass exterior. Any deposits observed in the fiberglass interior likely were chemical byproducts in the test or formed by chemical precipitation during the sample-drying process for ESEM/SEM analysis (see Figure 4-42). EDS analysis indicates that the deposits in Figure 4-42 contained insignificant amounts of phosphorus (see Figure 4-43), meaning that the deposits were distinct from the white gel found in this test.

Figure 4-36. ESEM image of a Test #3, Day 30, exterior high-flow fiberglass sample, magnified 100 times. (t3hifx33, 5/11/05)

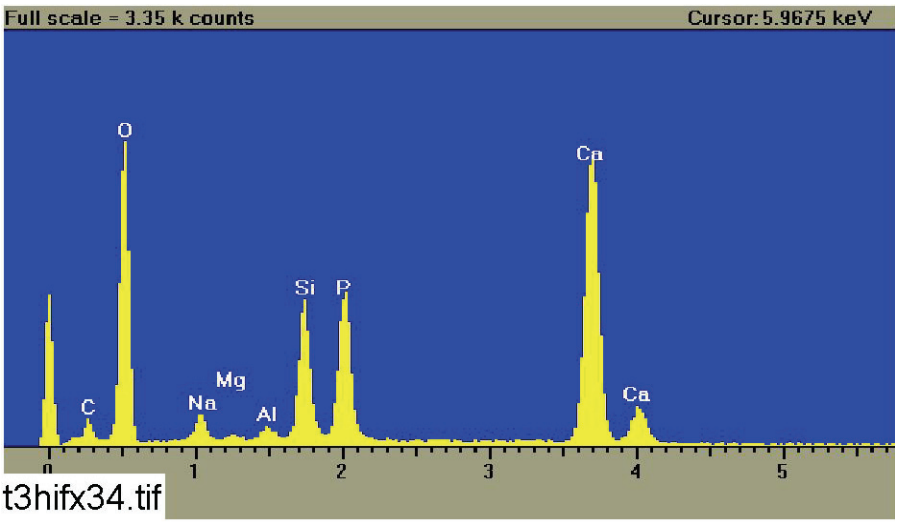

Figure 4-37. EDS counting spectrum for the large masses of particulate deposits shown in Figure 4-36. (t3hifx34, 5/11/05)

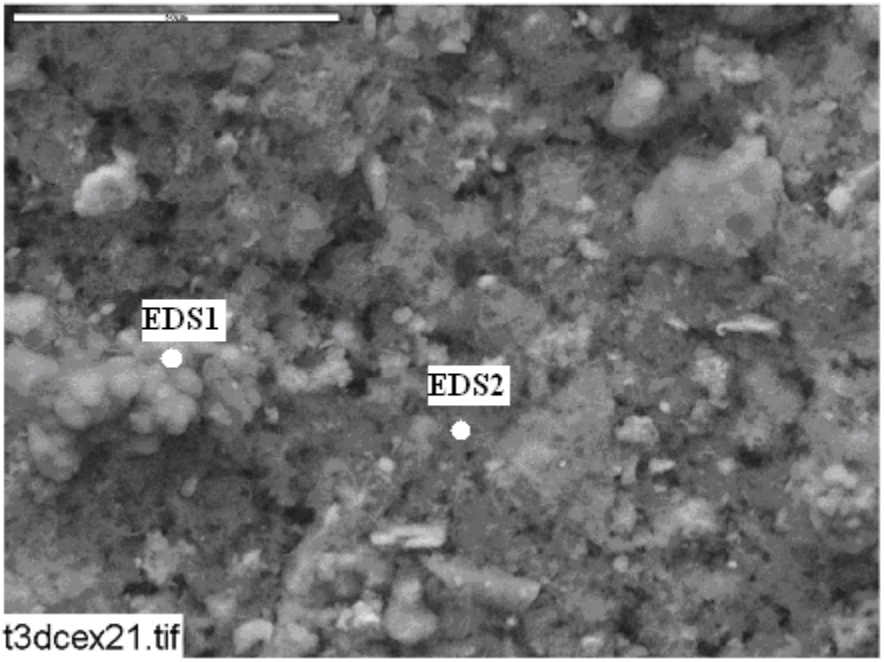

Figure 4-38. ESEM image of a Test #3, Day 30, exterior fiberglass sample on the drain collar (away from the drain screen), magnified 1000 times. (t3dcex21, 5/6/05)

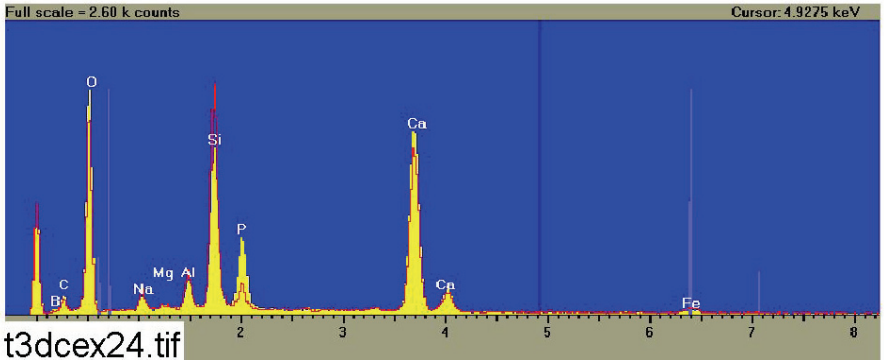

Figure 4-39. Comparison of EDS counting spectra between the light particle (EDS1, yellow) and the dark particle (EDS2, red) shown in Figure 4-38. (t3dcex24, 5/6/05)

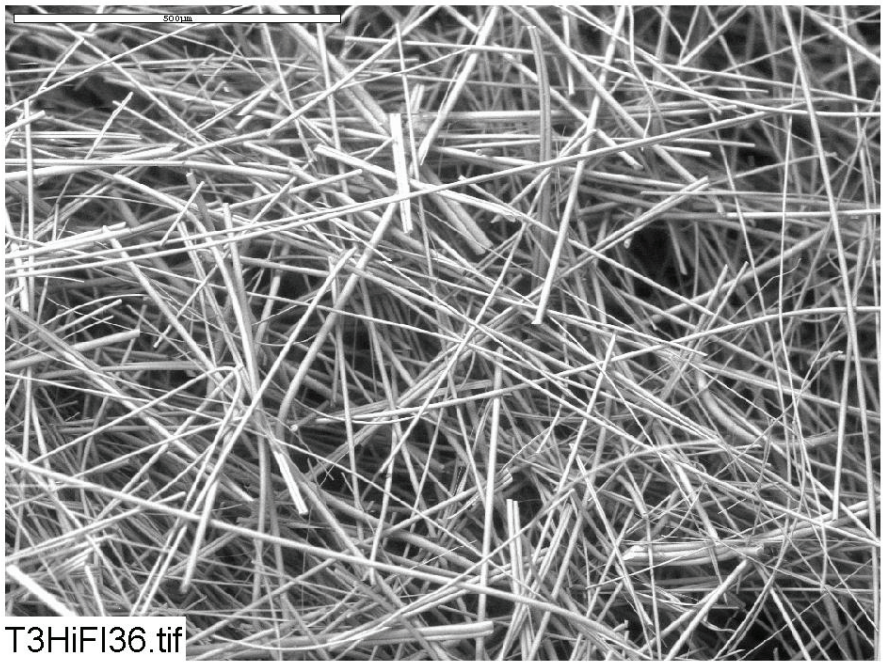

Figure 4-40. ESEM image of a Test #3, Day 30, interior high-flow fiberglass sample, magnified 100 times. (T3HiFI36, 5/11/05)

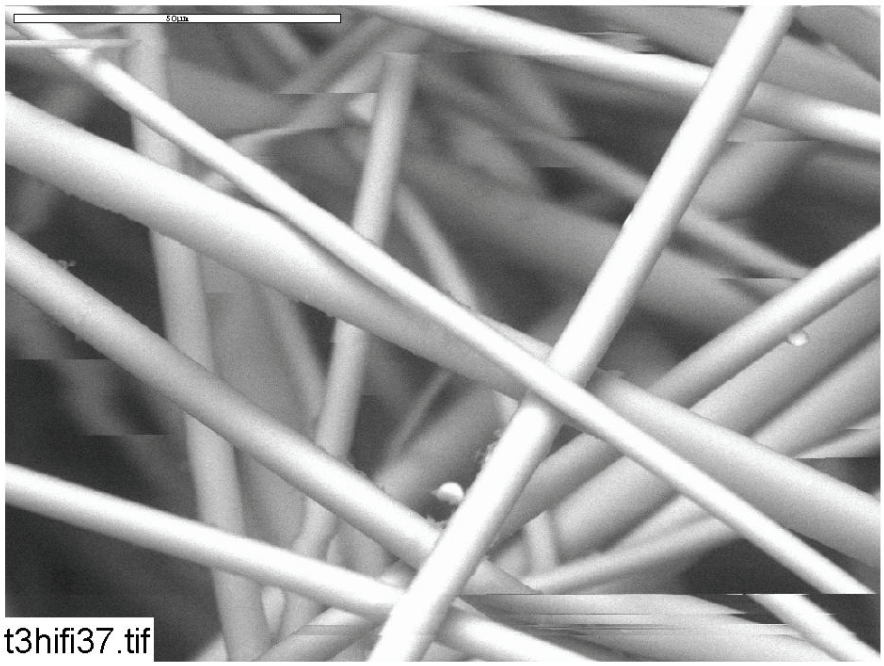

Figure 4-41. ESEM image of a Test #3, Day 30, interior high-flow fiberglass sample, magnified 1000 times. (t3hifi37, 5/11/05)

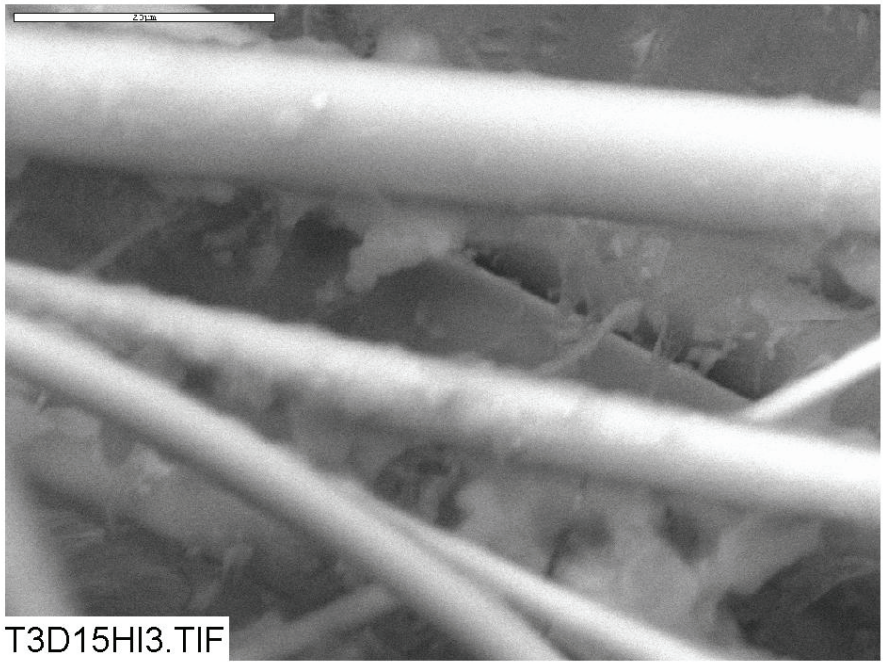

Figure 4-42. ESEM image of a Test #3, Day 15, high-flow interior fiberglass sample, magnified 2000 times. (T3D15HI3, 4/22/05)

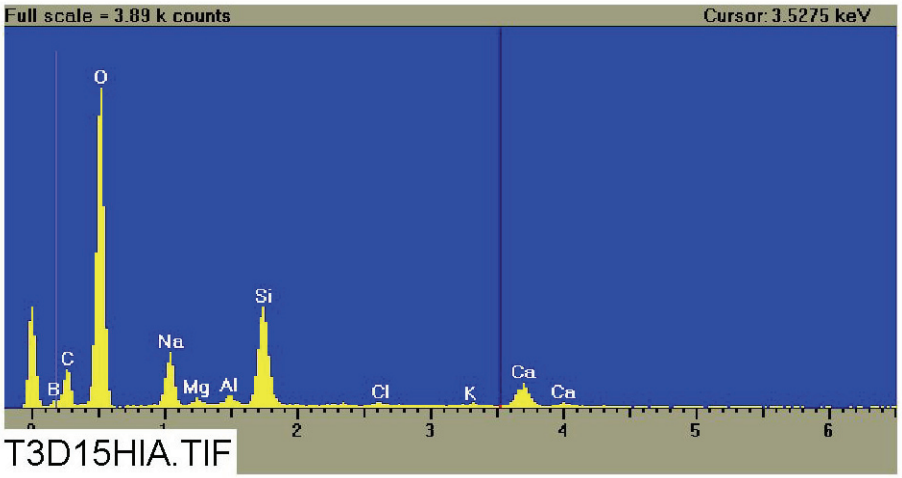

Figure 4-43. EDS counting spectrum for the flocculent deposits between the fibers on the ESEM image shown in Figure 4-42. (T3D15HIA, 4/22/05)

Test #4

The Test #4 fiberglass contained a large number of deposits, similar to Test #3. In Test #4, particulate deposits generally were found only on the exterior of the fiberglass, as shown in Figures 4-44, 4-45, 4-46, and 4-47. EDS analyses, as shown in Figure 4-48, indicate that these particulate deposits contain significant amounts of silicon and calcium, suggesting that they are from cal-sil debris. In contrast, the interior of fiberglass samples was relatively pristine, as shown in Figures 4-49 and 4-50. Only film deposits were observed. These deposits were likely formed by chemical precipitation when the samples were dehydrated. To investigate the formation of the film deposits, controlled experiments were performed by gently rinsing the interior fiberglass samples with several drops of RO water before an ESEM analysis was performed. Figures 4-51 and 4-52 show that after being rinsed with RO water, the film deposits disappeared from the fiberglass samples. These results suggest that the film is actually soluble, which is consistent with the explanation that the film was formed by chemical precipitation during the drying process of the fiberglass. In other words, although the ESEM analysis maintains samples in a moister state than does conventional SEM, the partial drying that took place during ESEM analysis was sufficient for some chemicals to precipitate and form the film deposits that were observed. This is consistent with the results obtained from the Test #1 flocculent deposits, which were presented earlier.

Figure 4-44. ESEM image, magnified 100 times, of a Test #4, Day 30, exterior high-flow fiberglass sample. (T4HFEx01.jpg)

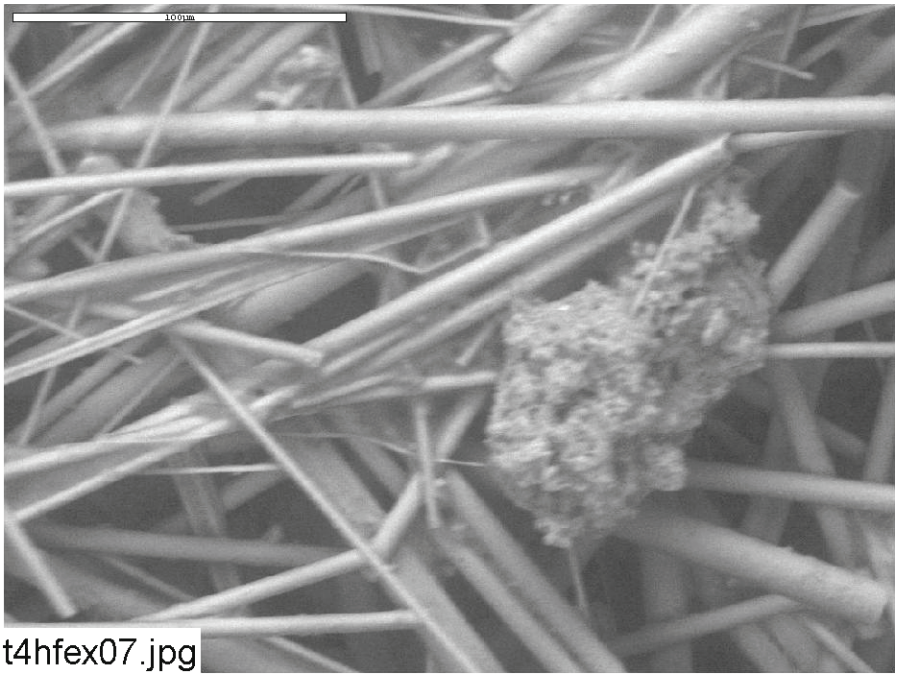

Figure 4-45. ESEM image, magnified 500 times, of a Test #4, Day 30, exterior high-flow fiberglass sample. (t4hfex07.jpg)

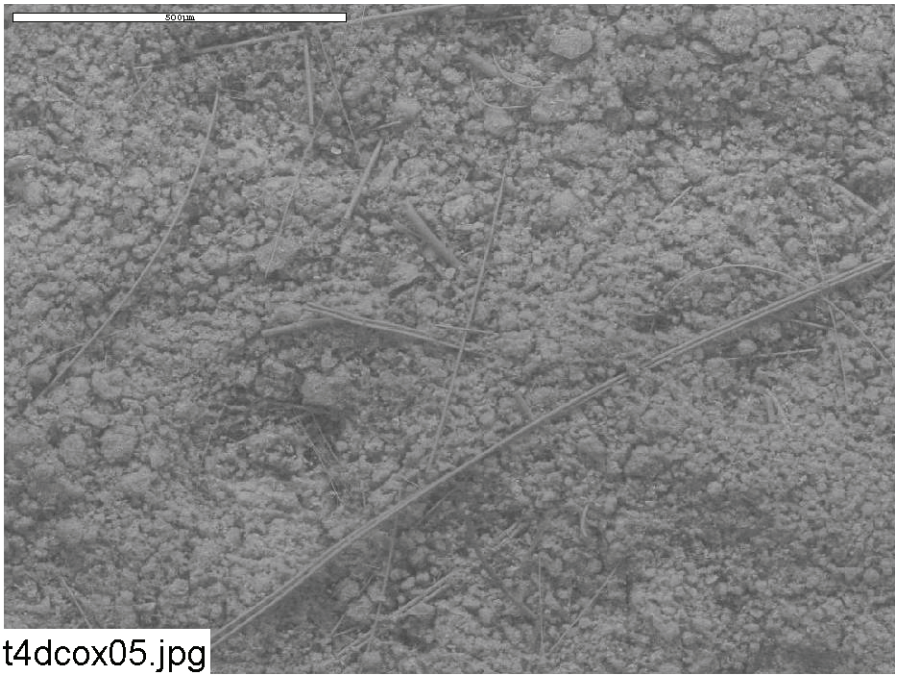

Figure 4-46. ESEM image, magnified 100 times, of a Test #4, Day 30, exterior fiberglass sample on the drain collar (away from the drain screen). (t4dcox05.jpg)

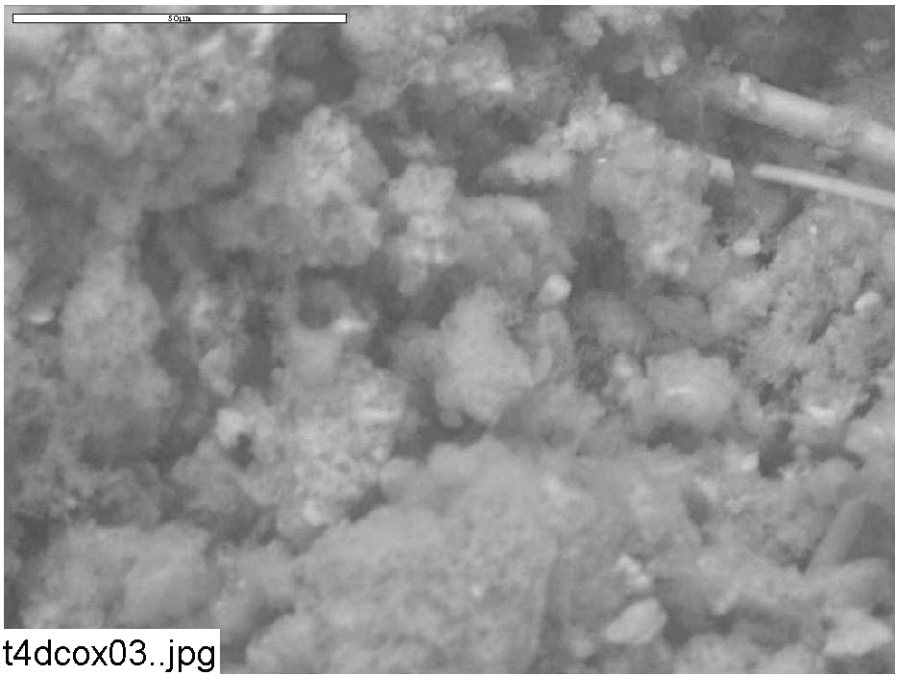

Figure 4-47. ESEM image, magnified 1000 times, of a Test #4, Day 30, exterior fiberglass sample on the drain collar (away from the drain screen). (t4dcox03.jpg)

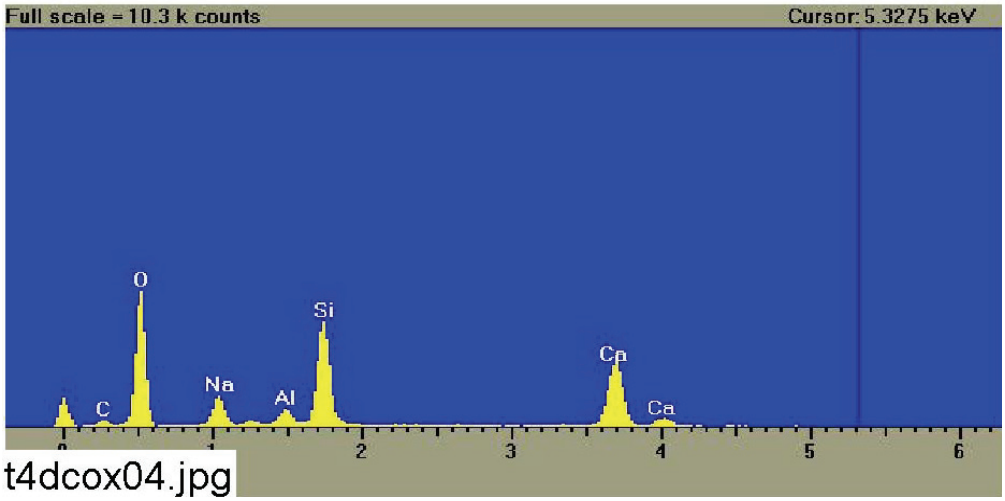

Figure 4-48. EDS counting spectrum for the large mass of particulate deposits on fiberglass shown in Figure 4-47. (t4dcox04.jpg)

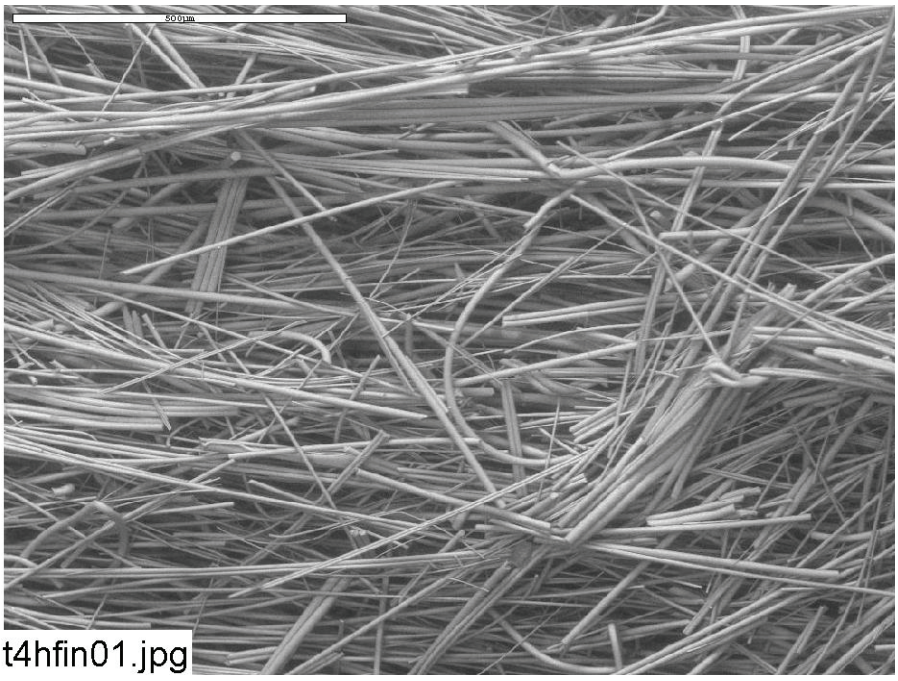

Figure 4-49. ESEM image, magnified 100 times, of a Test #4, Day 30, interior high-flow fiberglass sample. (t4hfin01.jpg)

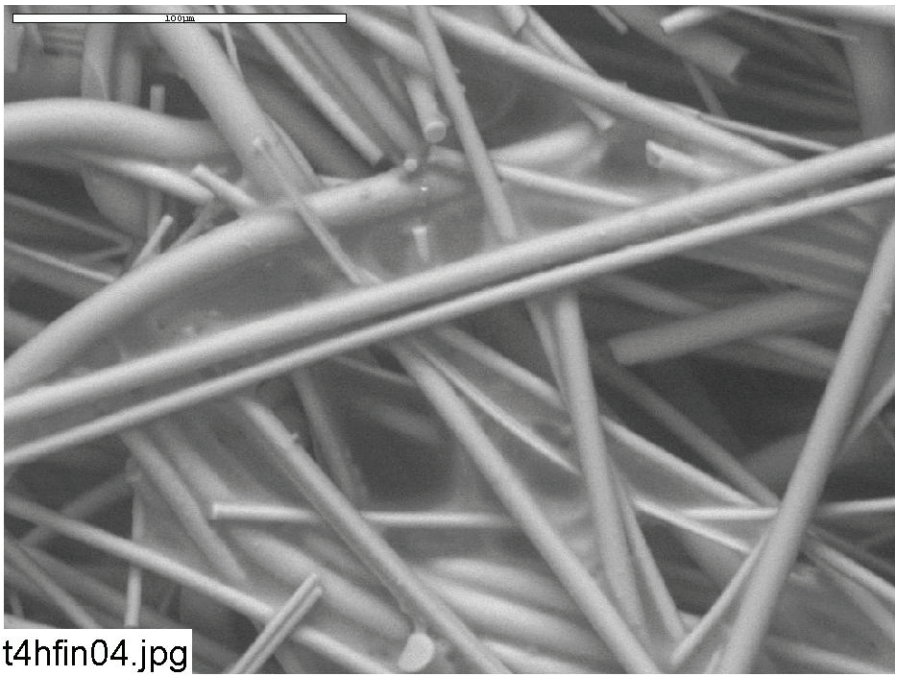

Figure 4-50. ESEM image, magnified 500 times, for a Test #4, Day 30, interior high-flow fiberglass sample. (t4hfin04.jpg)

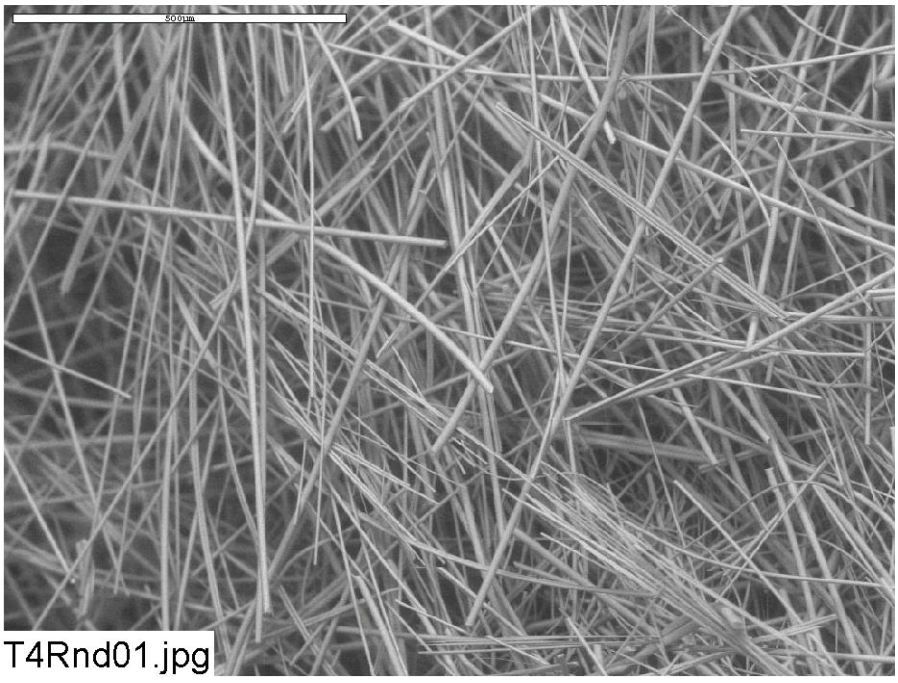

Figure 4-51. ESEM image, magnified 100 times, of a Test #4, Day 30, interior high-flow fiberglass sample. The sample was gently pre-rinsed with RO water. (T4Rnd01.jpg)

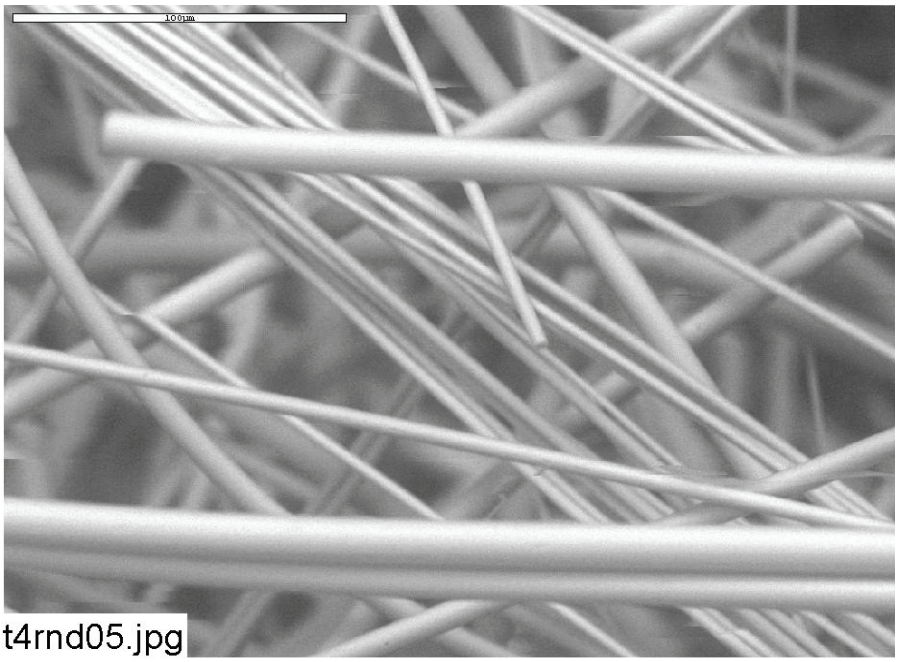

Figure 4-52. ESEM image, magnified 500 times, for a Test #4, Day 30, interior high-flow fiberglass sample. The sample was gently pre-rinsed with RO water. (t4rnd05.jpg)

Test #5

ICET Test #5 had the smallest amount of deposits in the fiberglass of any of the ICET tests. Day-30, high-flow fiberglass exterior samples are shown in Figures 4-53 and 4-54. The samples were relatively pristine, and they had the fewest particulate deposits. Similarly, interior samples shown in Figures 4-55, 4-56, and 4-57 were also relatively pristine. Only flocculent deposits were observed. The lack of deposits is likely because the smallest amount (compared to the other tests) of chemicals were added to the test solution. The flocculent deposits in the fiberglass interior were composed primarily of oxygen, sodium, calcium, magnesium, aluminum, and possibly silicon, as shown in Figure 4-58. These deposits likely were formed by chemical precipitation during dehydration of the samples, after the samples were removed from the tank, as demonstrated in the Test #4 results.

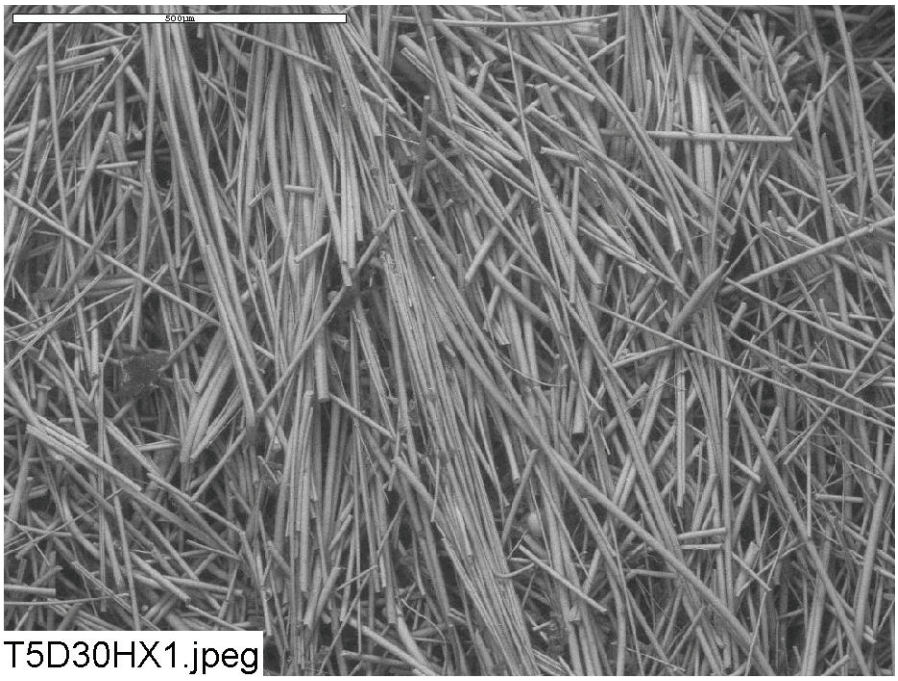

Figure 4-53. ESEM image, magnified 100 times, of a Test #5, Day 30, high-flow exterior fiberglass sample. (T5D30HX1.jpg)

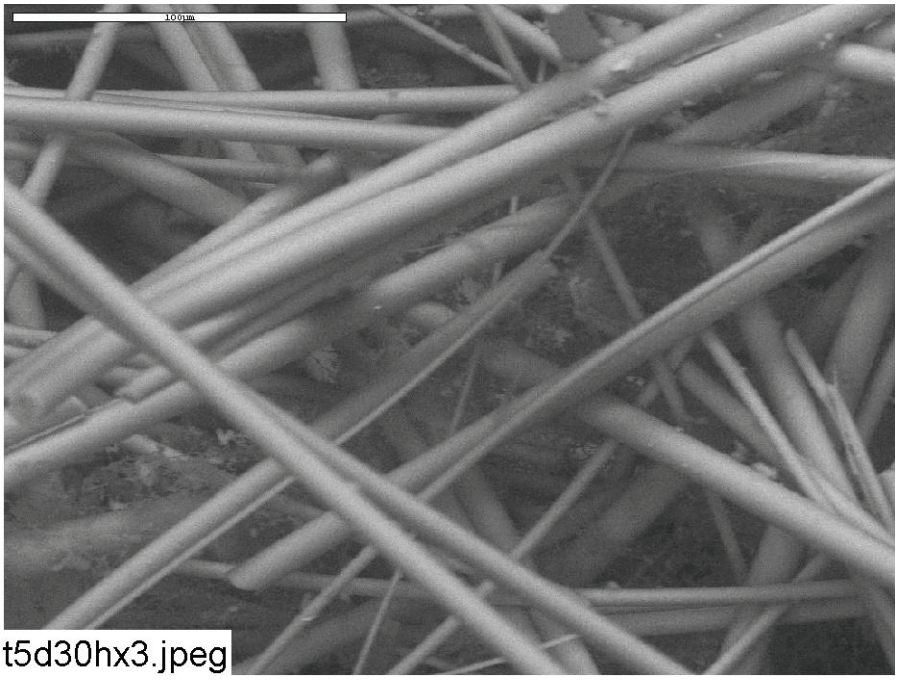

Figure 4-54. ESEM image, magnified 500 times, of a Test #5, Day 30, high-flow exterior fiberglass sample. (t5d30hx3.jpg)

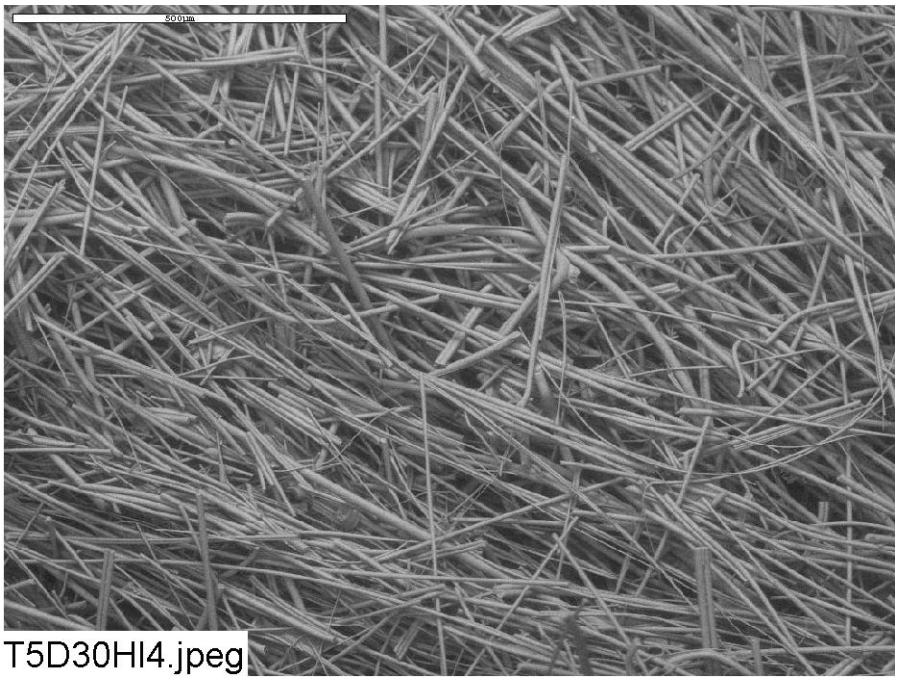

Figure 4-55. ESEM image, magnified 100 times, of a Test #5, Day 30, high-flow interior fiberglass sample. (T5D30HI4.jpg)

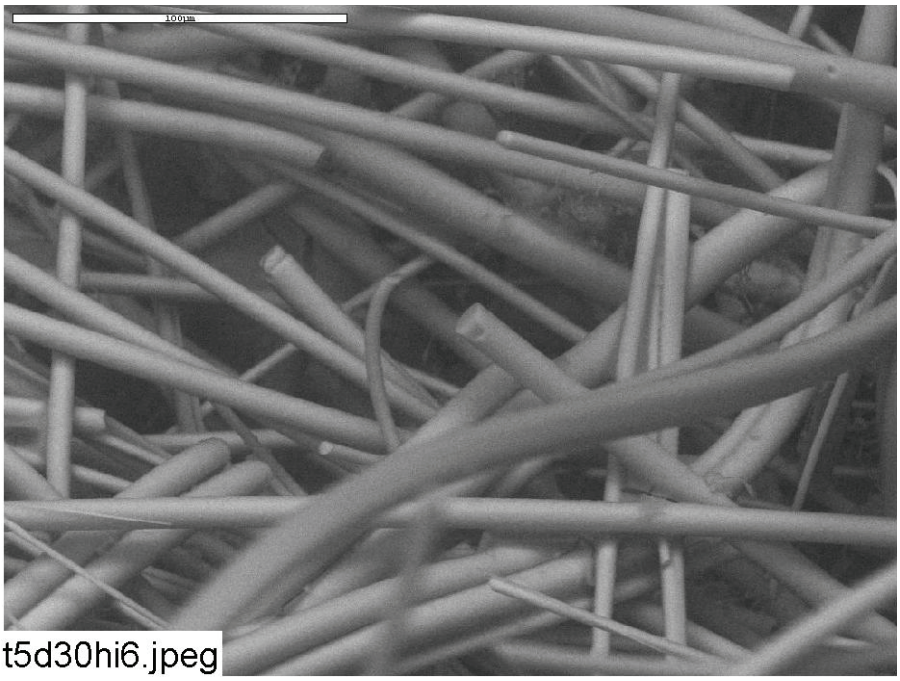

Figure 4-56. ESEM image, magnified 500 times, of a Test #5, Day 30, high-flow interior fiberglass sample. (t5d30hi6.jpg)

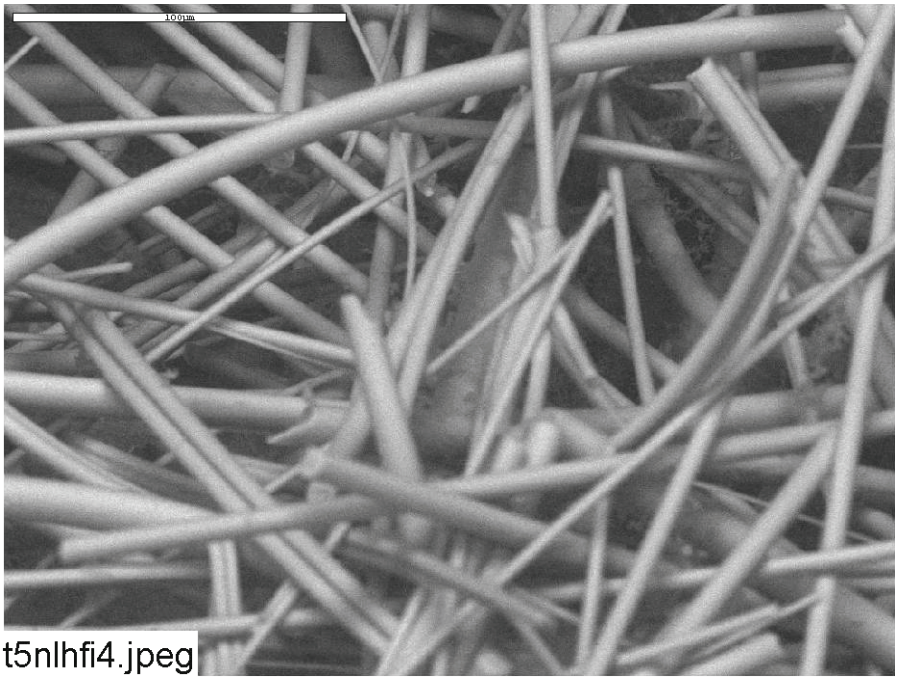

Figure 4-57. ESEM image, magnified 500 times, of a Test #5, Day 30 high-flow interior fiberglass sample in a nylon mesh.

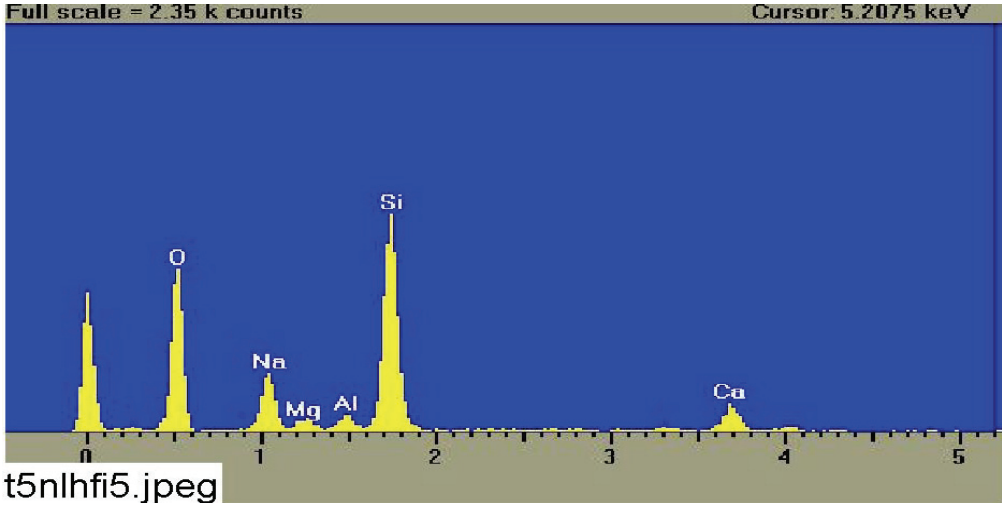

Figure 4-58. EDS counting spectrum for the deposits between the fibers shown in Figure 4-57.

4.2.2. Cal-Sil

In ICET Tests #3 and #4, 80% of the fiberglass was replaced with cal-sil. The cal-sil was divided into 4 size categories, in pieces that were roughly cubes. Of the total cal-sil, 14% was over 3 in., 19% was 1–3 in., 5% was less than 1 in., and 62% was "dust." The dust consisted of cal-sil pieces that were ground into a fine powder (Figure 2-6). With the exception of the dust, the cal-sil pieces were contained within SS mesh (Figure 2-5) and apportioned into submerged (75%

of the total) and unsubmerged (25% of the total) samples. The unsubmerged cal-sil was placed on the ends of suspended coupon racks. The dust was put into the tank solution before the test started.

The cal-sil released significant concentrations of calcium and silicate to the test solutions (see References 4 and 5). The released calcium and silicate may react with other chemical species in the test solutions, such as phosphate anions and aluminum cations. Because TSP was used in Test #3, a significant amount of phosphorus was found on the exterior of the submerged cal-sil samples in Test #3, in which phosphorus was likely present as calcium phosphate precipitate. However, almost no phosphorus was present in the interior of the submerged cal-sil. The result may be explained by the limited phosphate diffusion into the cal-sil interior. In Test #4, no phosphorus was found on the submerged cal-sil samples because TSP was not used. However, silicate released from cal-sil may have formed a passivation on the submerged aluminum coupon surface. As a result, the corrosion process was significantly decreased, as compared with Test #1 (see Section 4.4.3).

Unused Cal-Sil Samples

As a base-line analysis, the unused unbaked and baked cal-sil samples were examined by SEM, XRD, and XRF. Figures 4-59 and 4-60 show the SEM images of unused unbaked and baked cal-sil, respectively. The amount of fiber in baked cal-sil appears to be less than in unbaked cal-sil, suggesting that the fibers were organic material that was burned off during the baking process. XRD and XRF results show the crystal structure and the chemical composition of the unused unbaked and unused baked cal-sil samples. Based on XRD results, as shown in Figures 4-61 and 4-62, both unused unbaked and unused baked cal-sil samples contained crystalline substances of tobermorite [$Ca_{2.25}(Si_3O_{7.5}(OH)_{1.5})(H_2O)$] and calcite ($CaCO_3$). XRF results are presented in Table 4-5. The XRF analysis involves heating the sample to 80°C, during which all elements are oxidized to their highest oxidation state. Therefore, the results are reported as percent composition of oxides of various metals, but they give an indication of the elements that were detected in the sample. The results in Table 4-5 indicate that the dominant elements in cal-sil include silicon, calcium, and small amounts of aluminum, iron, sodium, manganese, titanium, phosphorus, and magnesium. As a result, silicon and calcium may be leaching out of the cal-sil to the test solution during Tests #3 and #4.

No significant difference was observed in elemental composition between unbaked and baked unused cal-sil, as shown in Table 4-6. Carbon content is an exception, because it cannot be quantified by XRF analysis. After being baked in a laboratory oven at 260°C for 72 hours, the unbaked cal-sil color changed from yellow to pink. The possible property changes of cal-sil after being baked include loss of water and oxidation of reduced species, such as organic carbon, Fe(0) and Fe(II), as well as possible mineral and crystal structural changes. Specifically, oxidation of Fe(0) and Fe(II) into Fe_2O_3 is likely responsible for the baked cal-sil turning pink.

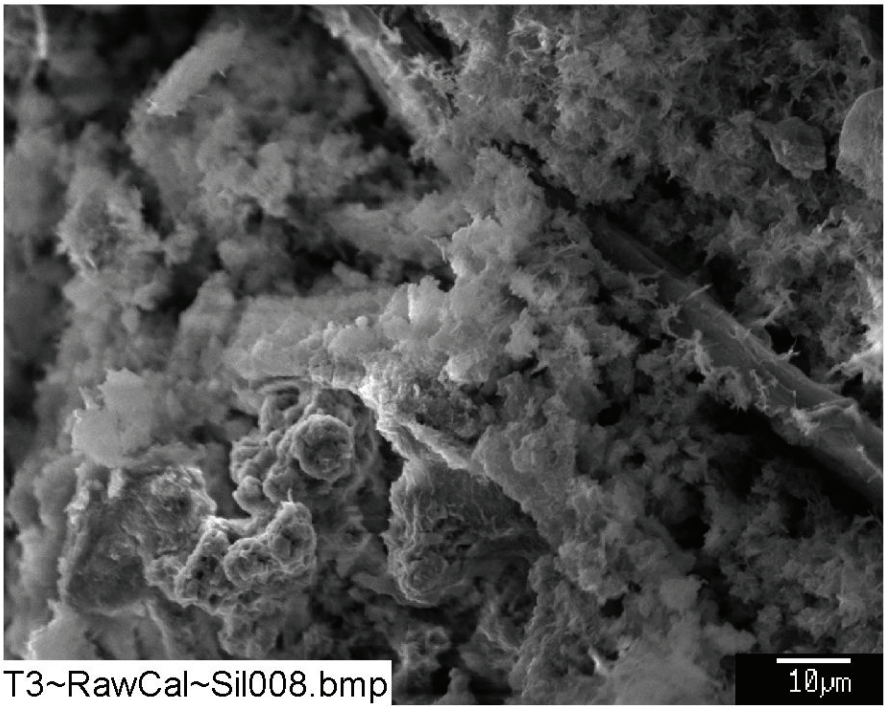

Figure 4-59. SEM image, magnified 1000 times, of an unused, unbaked cal-sil sample. (T3~RawCal_Sil008)

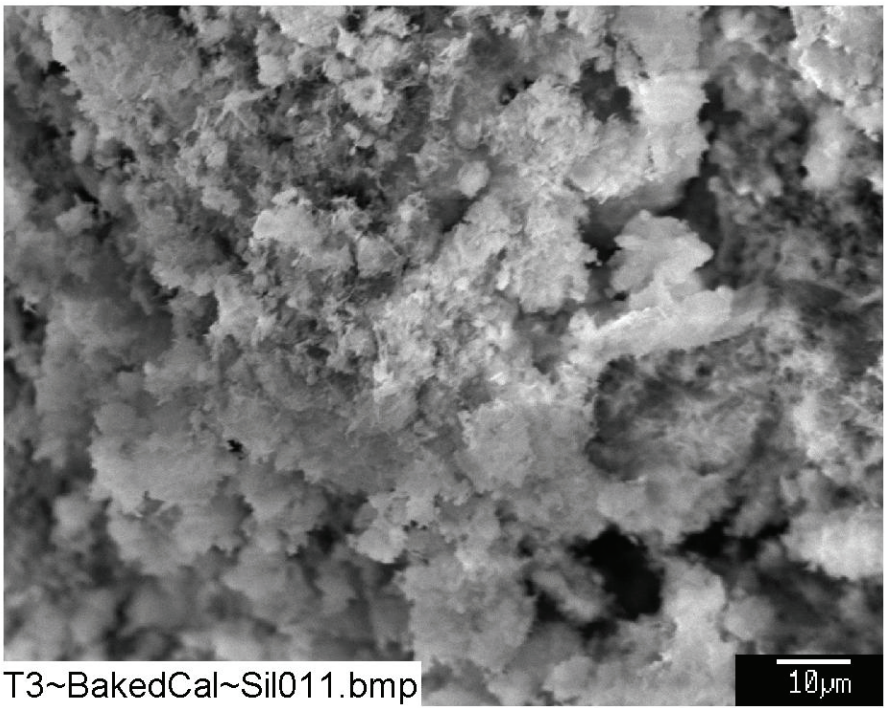

Figure 4-60. SEM image, magnified 1000 times, of an unused, baked cal-sil sample. (T3~BakedCal~Sil011)

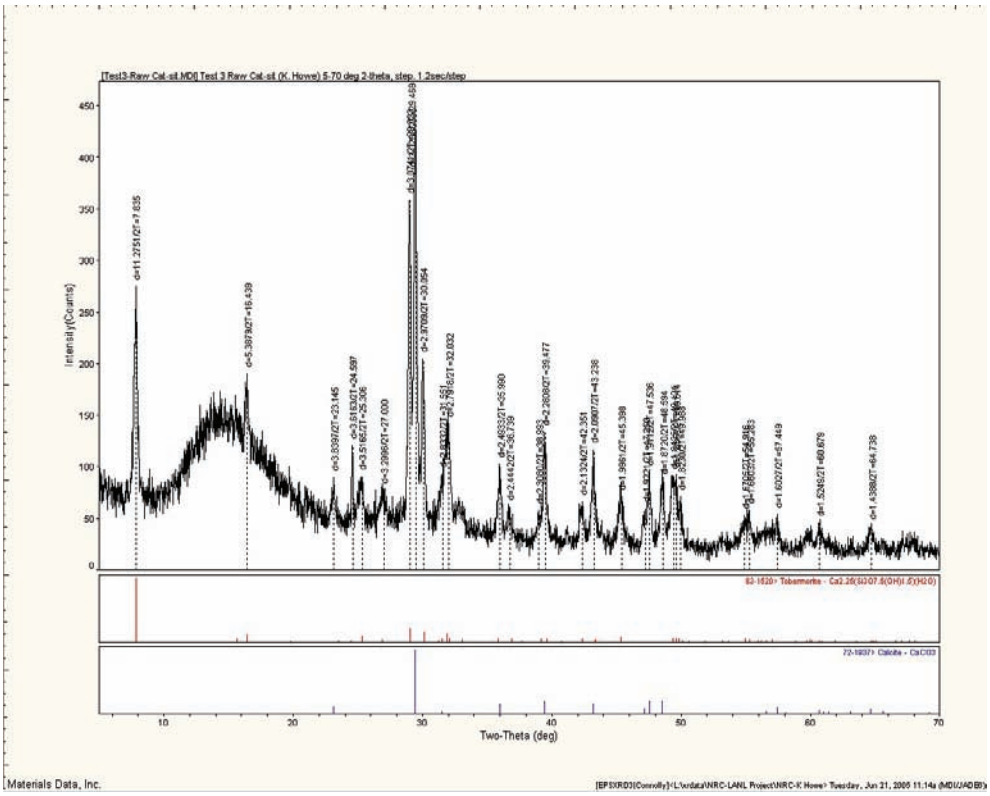

Figure 4-61. XRD results for the unused, unbaked cal-sil sample.

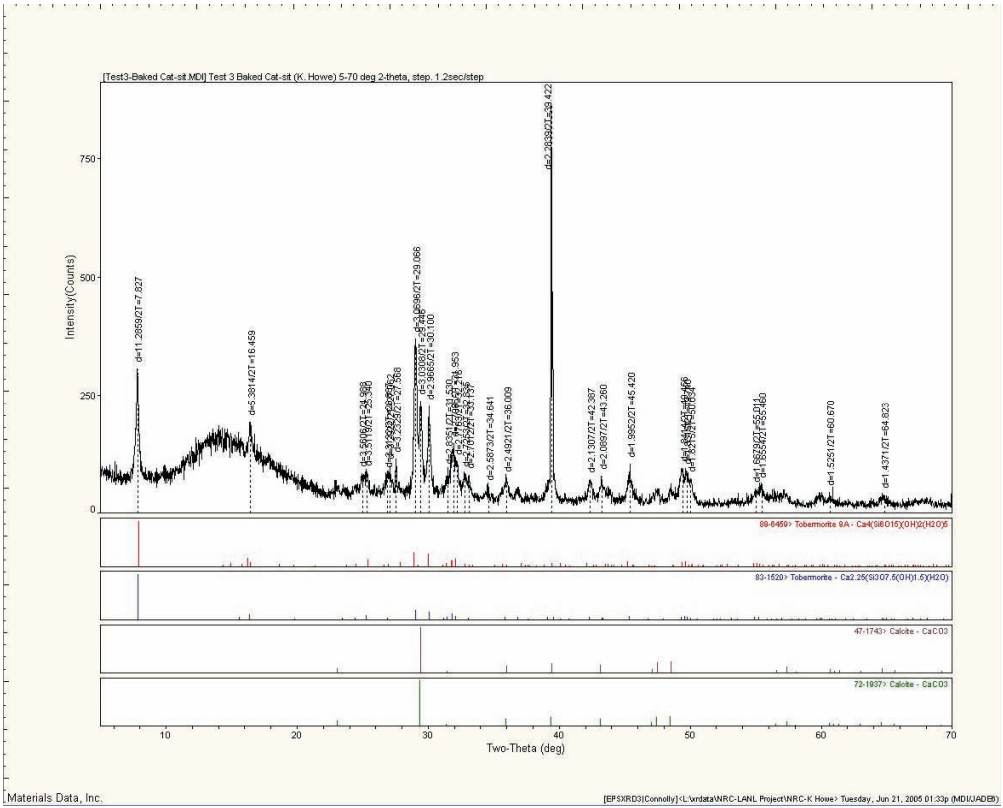

Figure 4-62. XRD results for the unused, baked cal-sil sample.

Table 4-6. Dry Mass Composition (%) of Unused Cal-Sil Samples by XRF Analysis

Compound	Unbaked Cal-Sil	Baked Cal-Sil
SiO_2	38.34	33.87
TiO_2	0.18	0.36
Al_2O_3	5.02	4.27
Fe_2O_3	2.54	2.07
FeO	0.00	0.00
MnO	0.06	0.05
MgO	0.79	1.35
CaO	34.76	34.66
Na_2O	2.32	2.27
K_2O	0.42	0.35
P_2O_5	0.15	0.12
$H_2O(-)$	0.35	0.56
$H_2O(+)CO_2$	18.75	1.59
Total	103.67	81.50

Test #3, Day 30, Submerged Cal-Sil Samples

TSP was injected into the test solution in Test #3 but not in Test #4. A Day-30 baked cal-sil sample that had been submerged in the high-flow region and a Day-30 unbaked cal-sil sample that had been submerged in the birdcage were examined. The exterior surface of the baked cal-sil samples from the high-flow region was examined by ESEM/EDS, and the results are shown in Figures 4-63, 4-64, and 4-65. These results show a significant amount of phosphorus, which is presumably because of the formation of a calcium phosphate precipitate. A comparison of Figures 4-64 and 4-65 indicates that Figure 4-64 has a phosphorus peak bigger than the silicon peak, and the situation is reversed in Figure 4-65. This suggests that the lighter-colored material in Figure 4-63 is predominantly the calcium phosphate precipitate on top of the cal-sil, whereas the darker-colored material is predominantly the background cal-sil. Smaller amounts of phosphorus were found on the exterior of the unbaked cal-sil in the birdcage sample, as shown in Figures 4-66 and 4-67, but the presence of phosphorus was still evident. However, almost no phosphorus was present in the interior of the unbaked cal-sil, as shown in Figures 4-68 and 4-69. The interior cal-sil sample was obtained by breaking a chunk of cal-sil in half and examining the interior surface with SEM. The lack of phosphorus may be explained by the limited phosphate diffusion into the cal-sil interior. The EDS results are used as evidence that phosphate may react with calcium in Test #3 and form calcium phosphate precipitates in the bulk solution and on the submerged cal-sil exterior surface, both baked and unbaked.

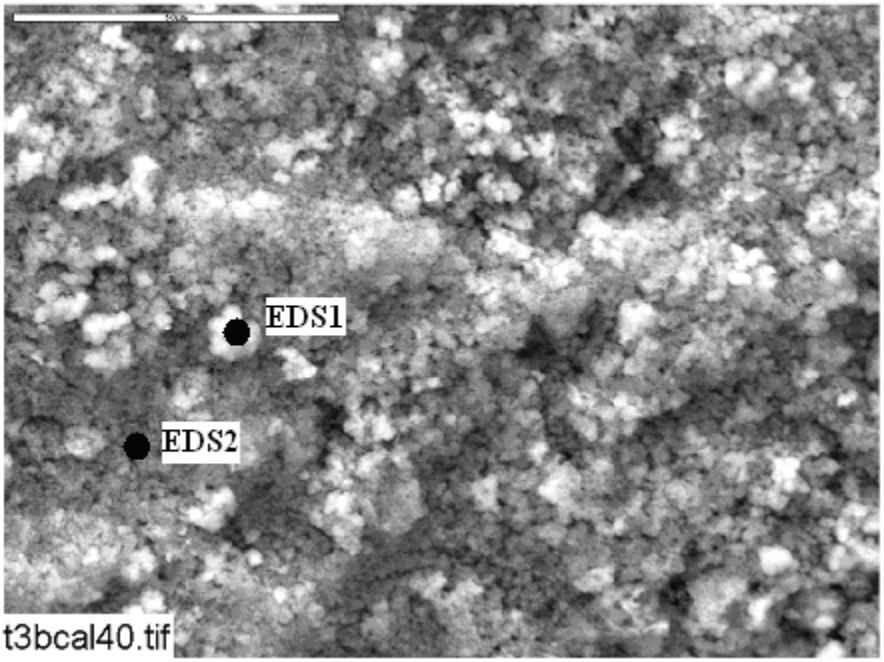

Figure 4-63. Annotated ESEM image, magnified 1000 times, of the exterior of a Test #3, Day 30, submerged high-flow baked cal-sil sample. (t3bcal40)

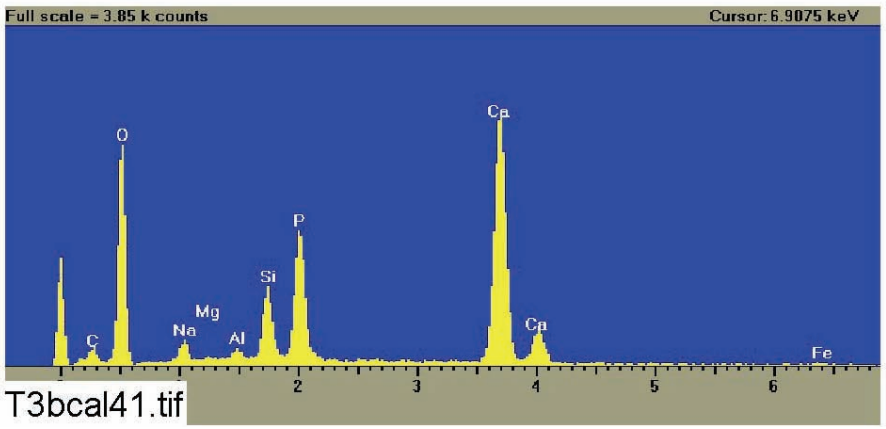

Figure 4-64. EDS counting spectrum for the light particles (EDS1) shown in Figure 4-63. (T3bcal41)

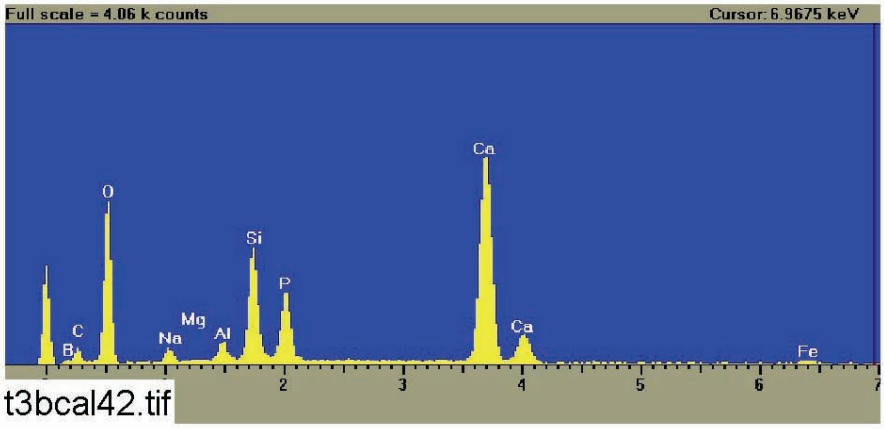

Figure 4-65. EDS counting spectrum for the dark particles (EDS2) shown in Figure 4-63. (t3bcal42)

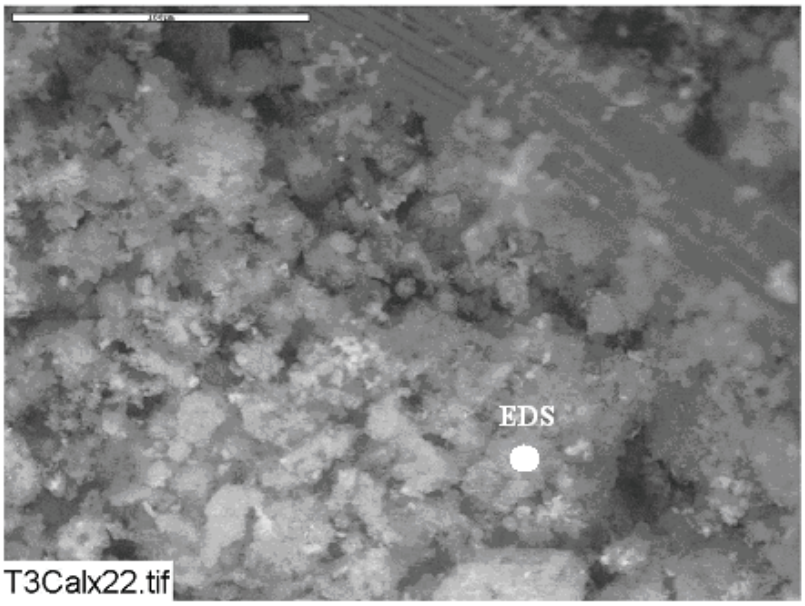

Figure 4-66. Annotated ESEM image, magnified 500 times, of the exterior of a Test #3, Day 30, unbaked cal-sil sample submerged in the birdcage. (T3Calx22)

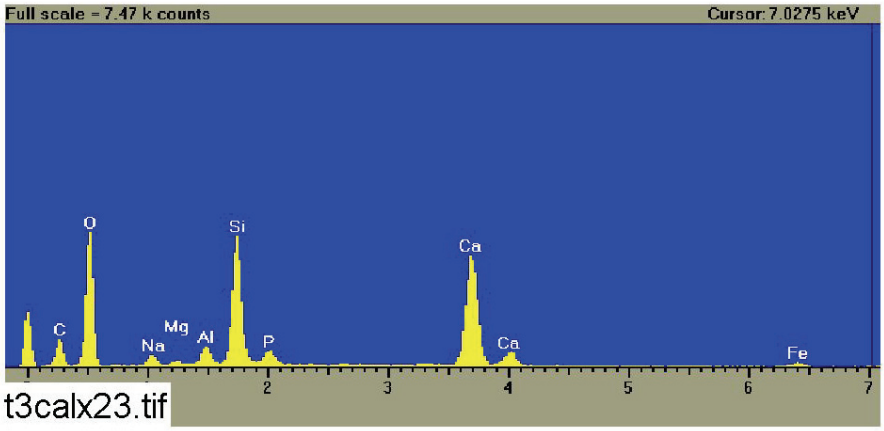

Figure 4-67. EDS counting spectrum for the particles shown in Figure 4-66. (t3calx23)

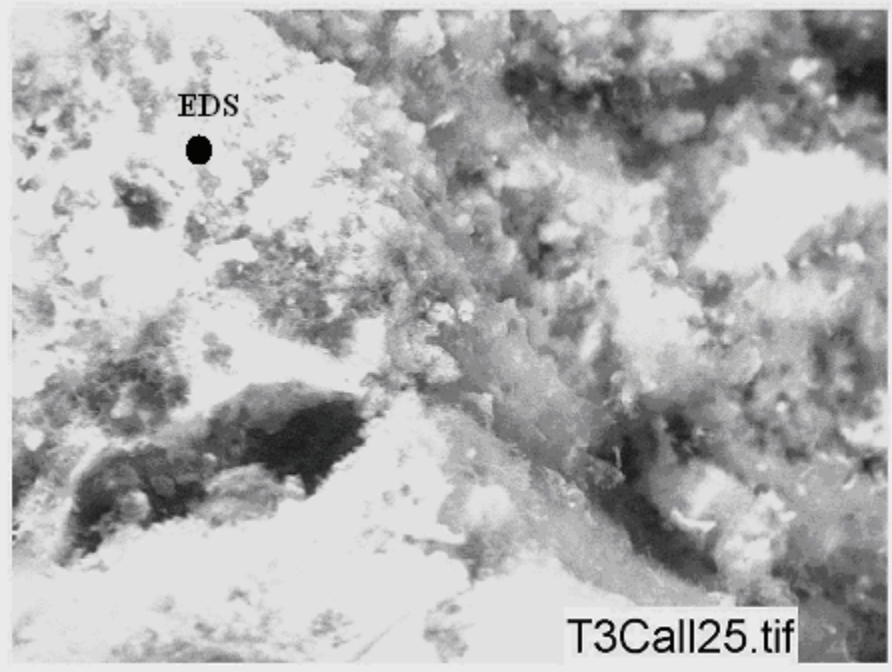

Figure 4-68. Annotated ESEM image, magnified 500 times, of the interior of a Test #3, Day 30, unbaked cal-sil sample submerged in the birdcage. (T3CalI25)

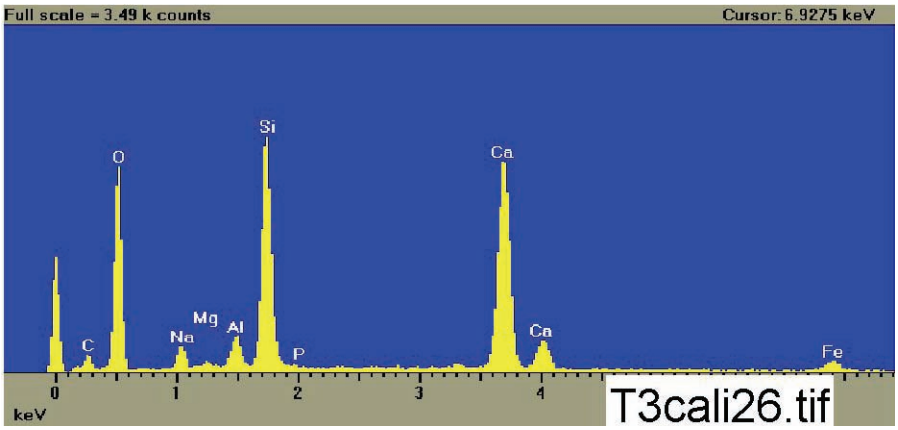

Figure 4-69. EDS counting spectrum for the particles shown in Figure 4-68. (T3cali26)

Test #4, Day 30, Submerged Cal-Sil Samples

No TSP was used in Test #4. Consequently, ESEM/EDS results showed no phosphorus on the exterior (Figures 4-70 and 4-71) or the interior cal-sil samples (Figures 4-72 and 4-73). The elements present in the Test #4 cal-sil are similar to the Test #3 cal-sil, with the exception of phosphorus and sodium. Phosphorus is observed on the exterior of the cal-sil samples in Test #3, but no phosphorus is observed in Test #4 because no TSP was used in Test #4. Comparing EDS results from Test #3 and Test #4, the sodium peak in Test #4 relative to other elements appears to be higher than in Test #3. This result is likely because of the relative differences in the aqueous sodium concentrations in the tests. In Test #3, 725 mg/L of sodium was added in the form of TSP, and in Test #4, 5520 mg/L of sodium was added in the form of NaOH. Residual sodium left on the samples during the drying and preparation process could leave the Test #4 samples with higher sodium than the Test #3 samples. In addition, sodium was present in solution as a dissolved ion throughout the duration of the tests (unlike phosphate) and was able to diffuse to the interior of the cal-sil (the cal-sil was essentially soaked in a sodium solution for 30 days) and so appears in relatively equal amounts in the interior and exterior.

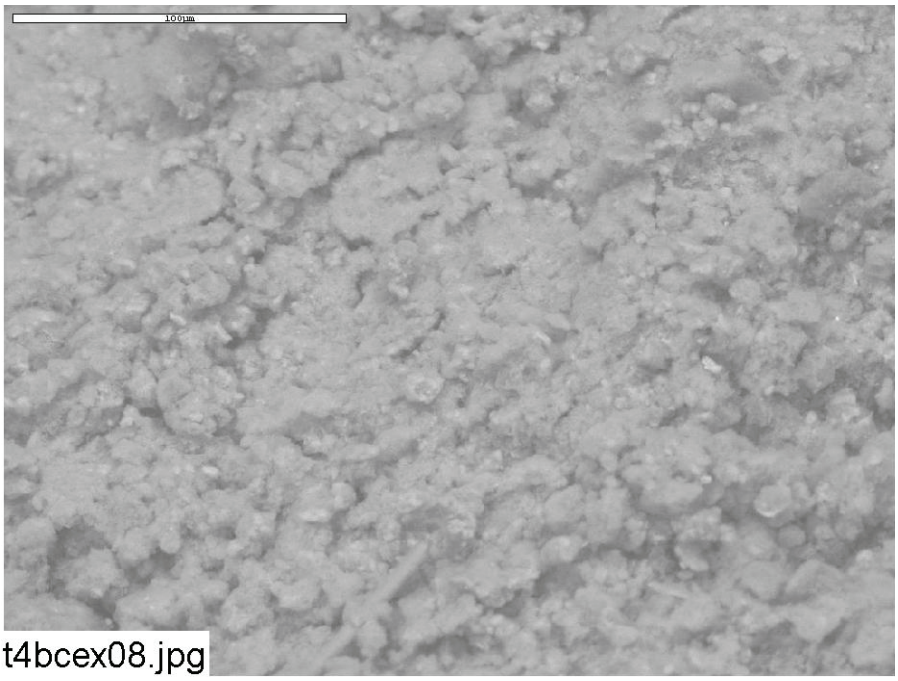

Figure 4-70. ESEM image, magnified 500 times, of a Test #4, Day 30, low-flow exterior baked cal-sil sample. (t4bcex08.jpg)

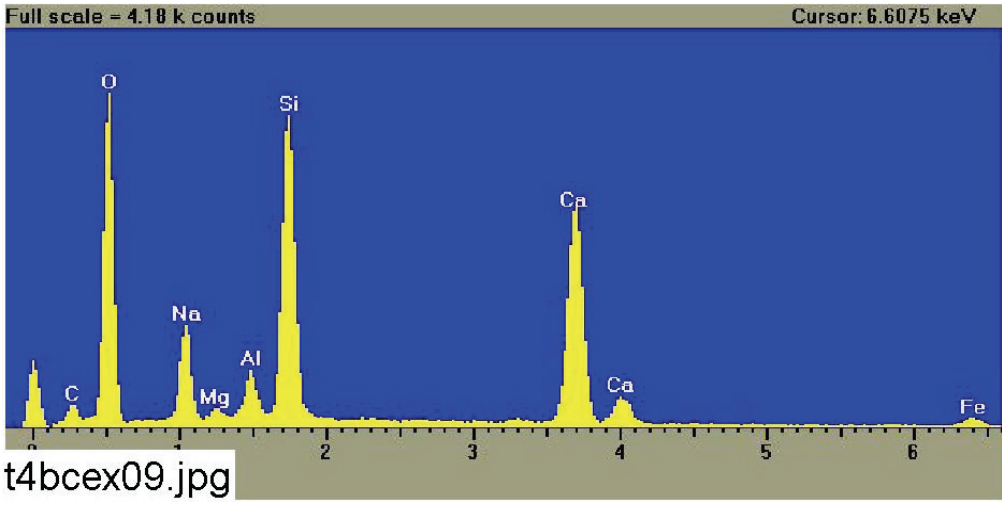

Figure 4-71. EDS counting spectrum for the whole image shown in Figure 4-70. (t4bcex09.jpg)

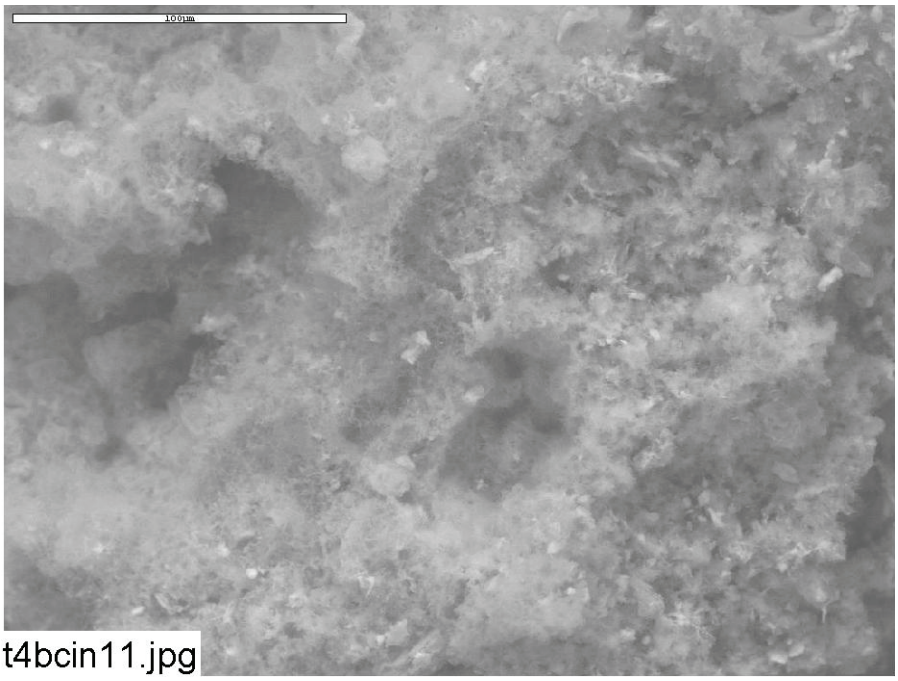

Figure 4-72. ESEM image, magnified 500 times, of a Test #4, Day 30, low-flow interior baked cal-sil sample. (t4bcin11.jpg)

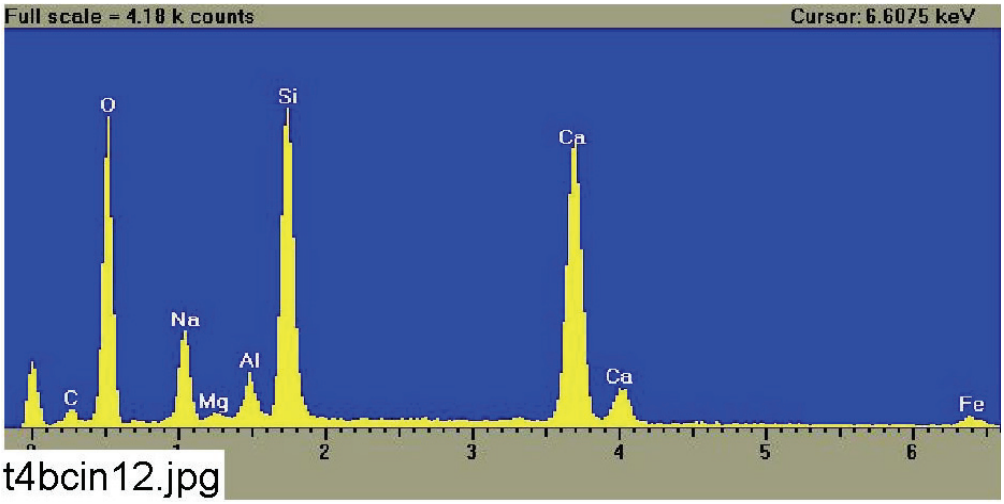

Figure 4-73. EDS counting spectrum for the whole image shown in Figure 4-72. (t4bcin12.jpg)

4.3. Sediment

According to photographic evidence and SEM/EDS analysis, the sediment samples from the five ICET tests were composed mainly of debris of insulation material (i.e., fiberglass and/or cal-sil), dirt, corrosion products, and chemical precipitates. However, because of the differences in solution conditions (i.e., pH and trisodium phosphate) and the insulation materials, the relative compositions and amounts of the sediments varied among the tests. As shown in Table 4-6, the